



國立臺灣大學理學院物理學系

碩士論文

Department of Physics

College of Science

National Taiwan University

Master Thesis

藉由熱輔助密度泛函對葉黃素類及其相關系統的

電子性質研究

A Thermally-assisted-occupation density functional theory study
of electronic properties of xanthophylls and its related systems

黃信評

Sin-Ping Huang

指導教授：蔡政達 博士

Advisor: Jeng-Da Chai, Ph.D.

中華民國 112 年 8 月

August, 2023

致謝



很開心終於能夠將論文撰寫完成，儘管研究上還有許多可以改進以及調整的地方，但無論如何總是完成了屬於自己的一份論文。

最需要感謝的是指導教授蔡政達教授，在我對研究主題感到迷茫時提供了許多協助，讓我能夠確立研究方向；也在我研究及論文撰寫的過程中持續給予幫助，使我在對於未來感到不安、對研究方向不確定時，使我不要慌張能夠專注在研究上。

另外要感謝兩位口試委員：林倫年主任跟趙聖德教授，感謝他們願意擔任口試委員，感謝他們在口試前後提供的協助，也感謝他們在口試中給予的各項批評與建議，讓我發現了研究中的不足之處，對於我在改善論文時助益良多。(In addition, I want to thank Dr. Hayashi and Dr. Chao for agreeing to attend my thesis defense, and thank you for your help before and after the defense. Your critic and opinion in the defense are so crucial to my research, it help me find the shortcoming of my research and help me to improve my thesis.)

也要感謝在臺大物理系求學的這幾年中在課堂上及課堂外所遇到的各式各樣的人事物，從大學部到現在即將從研究所畢業，過程中遇到的同學跟老師們都讓我在台大的生活更加精彩。

最後最後要感謝父母與家人的陪伴，感謝父母的經濟支持，讓我可以不用擔心金錢的問題專心投入在研究之中；感謝家人的陪伴，讓我在研究繁忙之際可以得到精神上的支持。

摘要

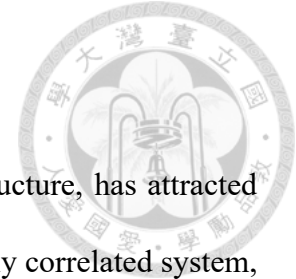


葉黃素類 (xanthophyll) 是類胡蘿蔔素 (carotenoid) 的其中一種類別，因其經常出現在健康保健食品中為最出名。如果想要使用傳統上最廣為使用的科恩-沈密度泛函理論 (Kohn-Sham density functional theory) 來處理葉黃素類，會因其為強關聯系統 (strongly correlated system) 而導致困難。所以我們使用熱輔助密度泛函理論 (thermally assisted occupation density functional theory) 來求得葉黃素類的相關化學性質。在本篇論文中我們針對四種在工業及學術文獻上較常出現的四種葉黃素類：蝦青素 (astaxanthin)，角黃素 (canthaxanthin)，葉黃素 (lutein) 和玉米黃素 (zeaxanthin) 及其相關系統做研究。相關系統是指我們將碳加入其碳鏈中使其結構中的碳鏈延長而得到的新化合物，我們會另外研究葉黃素類的相關系統是為了更加了解強關聯系統的性質。

我們利用熱輔助密度泛函理論得到了葉黃素類及其相關系統的下列化學性質：單重態與三重態之間的能量差 (singlet-triplet gap)，垂直游離能 (vertical ionization potential)，垂直電子親和力 (vertical electron affinity)，基本能隙 (fundamental Gap) 和對稱馮紐曼熵 (symmetrized von Neumann entropy) 等等。

關鍵字：葉黃素類，類胡蘿蔔素，熱輔助佔據密度泛函理論，強關聯系統

Abstract



Xanthophylls, a class of carotenoids containing oxygen in its structure, has attracted much attention due to its health-related effect. Because it is a strongly correlated system, we will encounter difficulties using Kohn-Sham density functional theory (KS-DFT) to study xanthophylls. In order to deal with those strongly correlated systems, we will apply the recently established thermally-assisted-occupation density functional theory (TAO-DFT), which has a great performance with strongly correlated systems and have a frequent usage with systems having radical nature. We put our interest in four types of xanthophylls: astaxanthin, canthaxanthin, lutein, and zeaxanthin. For a better understanding of the radical nature and the effect due to this nature, we also study their lengthen systems, in which we add carbon atoms in the conjugate bond and keep the terminal groups unchanged. The electronic properties we have interest in include singlet-triplet gap ($ST\ gaps$), vertical ionization potential (IP_V), vertical electron affinity (EA_V), fundamental gap (E_g), symmetrized von Neumann entropy (S_{vN}), and active orbital occupation numbers. We find that the singlet state is the ground state and that the energy difference between single and triplet become smaller when xanthophylls become longer. The stronger strongly correlated effect has also been found with longer xanthophylls with the proof from symmetrized von Neumann entropy and orbital occupation numbers.

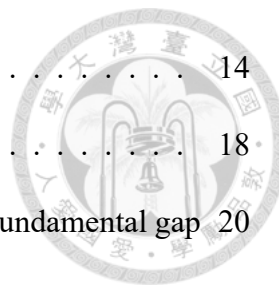
Key words: Xanthophyll, Carotenoid, Thermally-assisted-occupation density functional theory, Strongly correlated systems



Contents

謝辭	i
摘要	ii
Abstract	iii
Contents	iv
List of figures	vi
List of tables	x
1 Introduction	1
1.1 Carotenoids	1
1.2 Xanthophylls	3
2 Theoretical background	5
2.1 Density functional theory	5
2.2 Thermally-assisted-occupation density functional theory	7
2.3 Computational detail	10
3 Results	11

3.1	Singlet-Triplet gap	14
3.2	Energy difference between cis-trans isomerism	18
3.3	Vertical ionization potential & Vertical electron affinity & Fundamental gap	20
3.4	Symmetrized von Neumann entropy	26
3.5	Active orbital occupation numbers	28
4	Summary and future prospect	37
	Reference	39





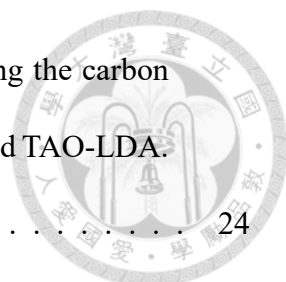
List of Figures

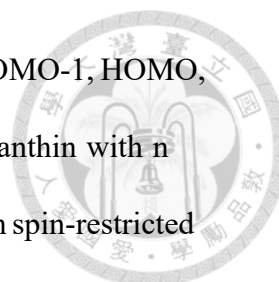
1.1	Different types of terminal groups	2
1.2	The structure of astaxanthin	3
1.3	The structure of canthaxanthin	3
1.4	The structure of lutein	3
1.5	The structure of zeaxanthin	4
3.1	The structure of n-lutein with n being the carbon number	12
3.2	The structure of cis-40-astaxanthin	13
3.3	The structure of trans-40-astaxanthin	13
3.4	The structure of cis-40-canthaxanthin	13
3.5	The structure of trans-40-canthaxanthin	13
3.6	The structure of cis-40-lutein	14



3.7	The structure of trans-40-lutein	14
3.8	The structure of cis-40-zeaxanthin	14
3.9	The structure of trans-40-zeaxanthin	14
3.10	Singlet-triplet energy gap of cis-n-xanthophyll with n being the carbon number. We performed the calculations with spin-unrestricted TAO-LDA. The basis set is 6-31G*.	15
3.11	Singlet-triplet energy gap of trans-n-xanthophyll with n being the carbon number. We performed the calculations with spin-unrestricted TAO-LDA. The basis set is 6-31G*.	16
3.12	Singlet state energy difference between cis-n-xanthophyll and trans-n-xanthophyll with n being the carbon number. We performed the calculations with spin-unrestricted TAO-LDA. The basis set is 6-31G*.	19
3.13	Vertical ionization potential of cis-n-xanthophyll with n being the carbon number. We performed the calculations with spin-unrestricted TAO-LDA. The basis set is 6-31G*.	21
3.14	Vertical ionization potential of trans-n-xanthophyll with n being the carbon number. We performed the calculations with spin-unrestricted TAO-LDA. The basis set is 6-31G*.	22
3.15	Vertical electron affinity of cis-n-xanthophyll with n being the carbon number. We performed the calculations with spin-unrestricted TAO-LDA. The basis set is 6-31G*.	23

3.16	Vertical electron affinity of trans-n-xanthophyll with n being the carbon number. We performed the calculations with spin-unrestricted TAO-LDA. The basis set is 6-31G*	24
3.17	Fundamental gap of cis-n-xanthophyll with n being the carbon number. We performed the calculations with spin-unrestricted TAO-LDA. The basis set is 6-31G*	25
3.18	Fundamental gap of trans-n-xanthophyll with n being the carbon number. We performed the calculations with spin-unrestricted TAO-LDA. The basis set is 6-31G*	26
3.19	Symmetrized von Neumann entropy of cis-n-xanthophyll with n being the carbon number. We performed the calculations with spin-unrestricted TAO-LDA. The basis set is 6-31G*	27
3.20	Symmetrized von Neumann entropy of trans-n-xanthophyll with n being the carbon number. We performed the calculations with spin-unrestricted TAO-LDA. The basis set is 6-31G*	28
3.21	Active orbital occupation numbers (HOMO-3, HOMO-2, HOMO-1, HOMO, LUMO, LUMO+1, LUMO+2, LUMO+3) of cis-n-astaxanthin with n being the carbon number. We performed the calculations with spin-restricted TAO-LDA. The basis set is 6-31G*	29
3.22	Active orbital occupation numbers (HOMO-3, HOMO-2, HOMO-1, HOMO, LUMO, LUMO+1, LUMO+2, LUMO+3) of trans-n-astaxanthin with n being the carbon number. We performed the calculations with spin-restricted TAO-LDA. The basis set is 6-31G*	30





3.23	Active orbital occupation numbers (HOMO-3, HOMO-2, HOMO-1, HOMO, LUMO, LUMO+1, LUMO+2, LUMO+3) of cis-n-canthalanthin with n being the carbon number. We performed the calculations with spin-restricted TAO-LDA. The basis set is 6-31G*	31
3.24	Active orbital occupation numbers (HOMO-3, HOMO-2, HOMO-1, HOMO, LUMO, LUMO+1, LUMO+2, LUMO+3) of trans-n-canthalanthin with n being the carbon number. We performed the calculations with spin-restricted TAO-LDA. The basis set is 6-31G*	32
3.25	Active orbital occupation numbers (HOMO-3, HOMO-2, HOMO-1, HOMO, LUMO, LUMO+1, LUMO+2, LUMO+3) of cis-n-lutein with n being the carbon number. We performed the calculations with spin-restricted TAO-LDA. The basis set is 6-31G*	33
3.26	Active orbital occupation numbers (HOMO-3, HOMO-2, HOMO-1, HOMO, LUMO, LUMO+1, LUMO+2, LUMO+3) of trans-n-lutein with n being the carbon number. We performed the calculations with spin-restricted TAO-LDA. The basis set is 6-31G*	34
3.27	Active orbital occupation numbers (HOMO-3, HOMO-2, HOMO-1, HOMO, LUMO, LUMO+1, LUMO+2, LUMO+3) of cis-n-zeaxanthin with n being the carbon number. We performed the calculations with spin-restricted TAO-LDA. The basis set is 6-31G*	35
3.28	Active orbital occupation numbers (HOMO-3, HOMO-2, HOMO-1, HOMO, LUMO, LUMO+1, LUMO+2, LUMO+3) of trans-n-zeaxanthin with n being the carbon number. We performed the calculations with spin-restricted TAO-LDA. The basis set is 6-31G*	36



List of Tables

3.1	Singlet and triplet state energy (Hartee) and the ST-gap (kcal/mol) for cis-n-astaxanthin and cis-n-canthaxanthin, where n is the carbon number. We performed the calculations with spin-unrestricted TAO-LDA. The basis set is 6-31G*	17
3.2	Singlet and triplet state energy (Hartee) and the ST-gap (kcal/mol) for cis-n-lutein and cis-n-zeaxanthin, where n is the carbon number. We performed the calculations with spin-unrestricted TAO-LDA. The basis set is 6-31G*	18



Chapter 1

Introduction

1.1 Carotenoids

Carotenoids are organic pigments that can color the world with yellow, orange, and red. It give color to flowers, fruit, vegetables and so much more. We can find carotenoids in various plants and there are various kinds of carotenoids exist in nature, in fact, more than one thousand types of carotenoids have been reported in the literature nowadays.[1] Carotenoids have attracted public attention recently mainly due to their use in feed additives, food coloring, and nutritional supplements.[2][3][4]

The structure of a carotenoids molecule have a conjugates carbon double bond and terminal groups in both end. The length of carbon bond and the different combinations of terminal groups will produce different molecules with various chemical properties. The length of conjugated carbon double bond is also a huge factor to the properties of carotenoids molecules. The great majority of them have a carbbon bond with 40 carbon atoms. We will refer to these molecules as C40 carotenoids, the number indicate the number of carbon atoms. The conjugated carbon double bond served as the chromophore

system, which will absorb the light with a wavelength range from 400 nm to 500 nm, as a result red, orange, and yellow are the colors we can see from carotenoids. There are seven types of terminal groups (β , γ , ϵ , κ , ϕ , χ , ψ), the basic structures of them are shown in the figure 1.1.[1][2][3]

There are two categories of carotenoids: carotenes and xanthophylls, by whether there are oxygen atoms exist in their structure. Carotenes molecules do not have oxygen in the structure, while xanthophylls molecules have oxygen in the structure, normally in their terminal groups. The terminal groups of xanthophylls come from naturally occurred enzymatic reaction.[1] Carotenes and xanthophylls both have widely usage in research field and industry. Some examples of carotenes are α -carotene, β -carotene and lycopene; and examples of xanthophylls are lutein and astaxanthin.

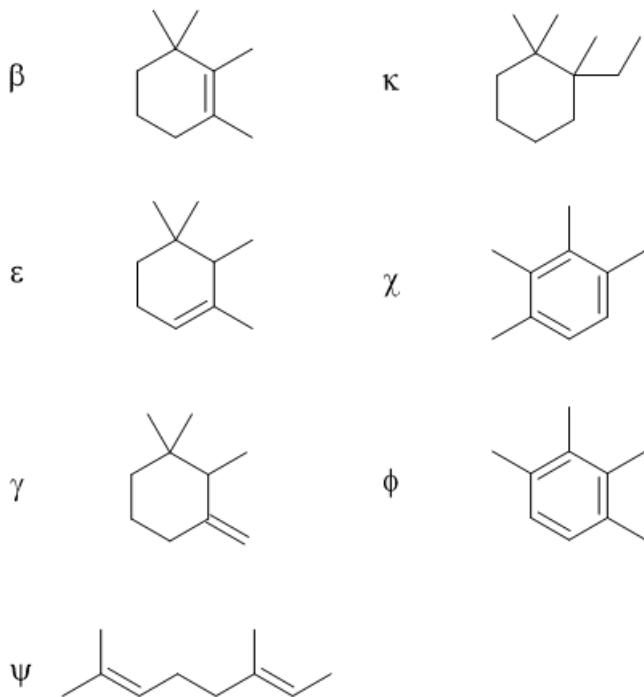


Figure 1.1: Different types of terminal groups

1.2 Xanthophylls

There are more than hundred types of xanthophylls, between them we choose four types of xanthophylls: astaxanthin ($C_{40}H_{52}O_4$), canthaxanthin ($C_{40}H_{52}O_2$), lutein ($C_{40}H_{56}O_2$), zeaxanthin ($C_{40}H_{56}O_2$) for our study. Their structure are displayed in the following figure.

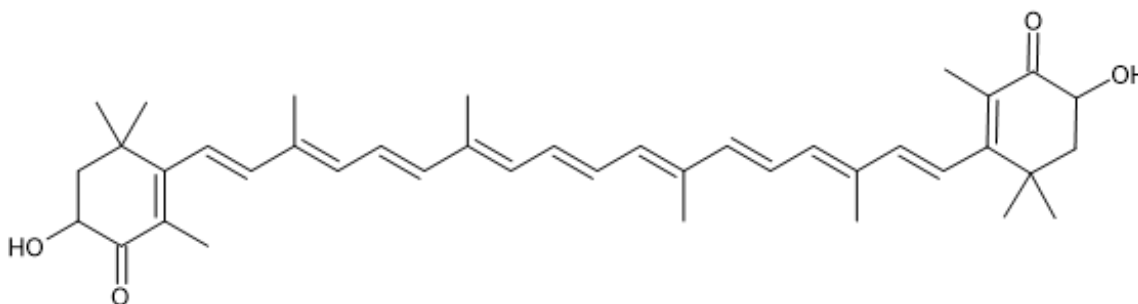


Figure 1.2: The structure of astaxanthin

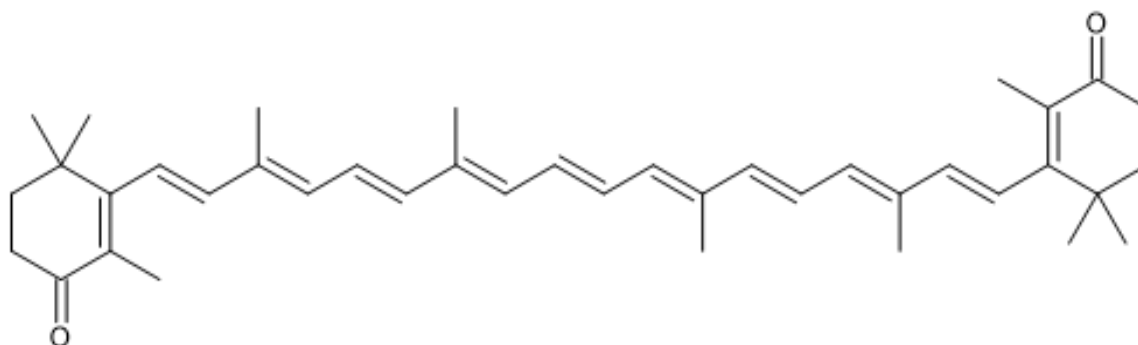


Figure 1.3: The structure of canthaxanthin

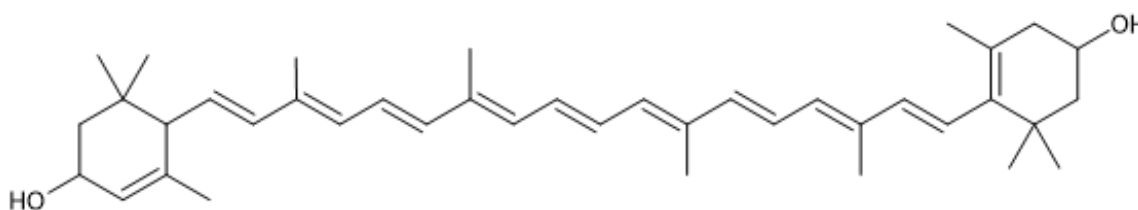


Figure 1.4: The structure of lutein

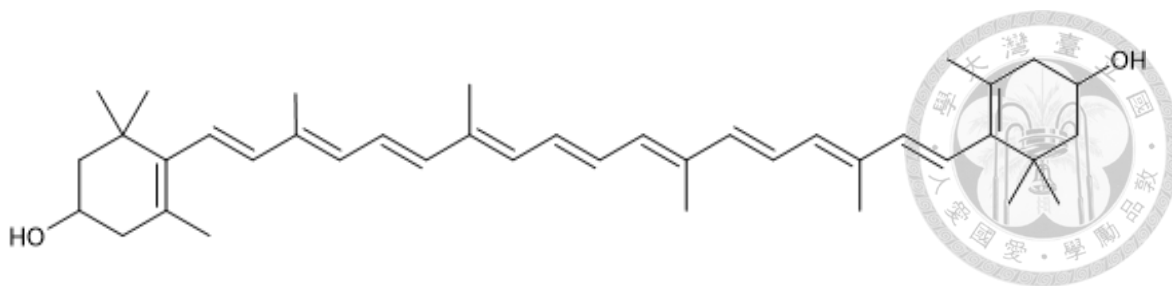


Figure 1.5: The structure of zeaxanthin

In xanthophylls oxygen will present in the carbonyl groups (C=O) or in the hydroxyl group (-OH) as we can see from the structure above. In astaxanthin oxygen present in both functional group; in canthaxanthin oxygen present in carbonyl group; in lutein and zeaxanthin oxygen present in hydroxyl group. These four xanthophylls are all frequently used in various fields of industry and have been synthesized on an industrial scale in the nutraceutical industry. Astaxanthin and canthaxanthin have a combined share over half the market of carotenoids due to its usage in animal feeding additive. For another usage, they can be the key to some disease's treatment. For example, astaxanthin has the potential to use in the treatment of skin cancer, cardiovascular disease ,and prostatic cancer.[2][5][6]

Xanthophylls come from various source in the nature, we can get astaxanthin from source including microalgae (e.g. *Haematococcus pluvialis*, *Euglena sanguinea*, *Chlamydomonas nivalis*), bacteria (e.g. *Paracoccus carotinifaciens*, *Agrobacterium auratiacum*, *Brevundimonas sp.*), plant (e.g. *Adonis annua*, *Adonis aestivalis*), and yeast (e.g. *dendrorhous*). Canthaxanthin can be found from *Cantharellus cinnabarinus*, a fungus with red color. Lutein and zeaxanthin can be found from places like wheat endosperm, sweet potato ,and the macula. Macula is a yellow spot in the retina, hence the yellow color. Lutein and zeaxanthin are believe to benefit human's vision; therefore, they can be found in some nutritional supplements that claim to improve visual function of human. [2][7]



Chapter 2

Theoretical background

2.1 Density functional theory

Kohn-Sham scheme

For the real system the electrons will have interaction with each other, which will cause an hard-to-deal energy term. In 1965 Kohn and Sham propose the Kohn-Sham scheme in which we have an non-interacting Kohn-Sham reference frame with an effective potential. The effective potential is set to make the ground state electron density in this scheme be the same as the real system.[5]

In the real system, the Hamiltonian is

$$\hat{H} = \hat{T} + \hat{V}_{ext} + \hat{V}_{ee} \quad (2.1)$$

and the energy functional is

$$E[\rho] = \int \rho(\vec{r}) V_{ext}(\vec{r}) d\vec{r} + F[\rho] \quad (2.2)$$

where

$$F[\rho] = \langle \Phi | \hat{T} + \hat{V}_{ee} | \Phi \rangle = T[\rho] + u_{ee}[\rho] = T_s[\rho] + E_H[\rho] + E_{xc}[\rho] \quad (2.3)$$

Hartree energy is

$$E_H[\rho] = \frac{1}{2} \int d\vec{r}_1 \int d\vec{r}_2 \frac{\rho(\vec{r}_1)\rho(\vec{r}_2)}{|\vec{r}_1 - \vec{r}_2|} \quad (2.4)$$

exchange-correlation energy is

$$E_{xc}[\rho] = \int \epsilon_{xc}(\vec{r}) d\vec{r} \quad (2.5)$$

and the Euler equation is

$$\mu = \frac{\delta E[\rho]}{\delta \rho} = V_{ext}(\vec{r}) + \frac{\delta T_s[\rho]}{\delta \rho} + \frac{\delta E_H[\rho]}{\delta \rho} + \frac{\delta E_{xc}[\rho]}{\delta \rho} \quad (2.6)$$

where

$$\frac{\delta E_H[\rho]}{\delta \rho} = V_H(\vec{r}(\rho)) \quad \text{and} \quad \frac{\delta E_{xc}[\rho]}{\delta \rho} = V_{xc}(\vec{r}(\rho)) \quad (2.7)$$

In the reference system, the Hamiltonian is

$$\hat{H} = \hat{T} + \hat{V}_{eff}$$

and the energy functional is

$$E_s[\rho_s] = \int \rho_s(\vec{r}) V_{eff}(\vec{r}) d\vec{r} + F_s[\rho_s] \quad (2.8)$$

where

$$F_s[\rho_s] = \langle \Phi | \hat{T} | \Phi \rangle = T_s[\rho_s] \quad (2.9)$$

and the Euler equation is

$$\mu_s = \frac{\delta E_s[\rho_s]}{\delta \rho_s} = V_{eff}(\vec{r}) + \frac{\delta T_s[\rho_s]}{\delta \rho_s} \quad (2.10)$$

By subtract both Euler equation we get the relation, where we can get $V_{eff}(\vec{r})$ from a given $\rho(\vec{r})$

$$V_{eff}(\vec{r}) = V_{ext}(\vec{r}) + V_H(\vec{r}(\rho)) + V_{xc}(\vec{r}(\rho)) + \mu_s - \mu$$

$$= V_{ext}(\vec{r}) + \frac{\delta E_H[\rho]}{\delta \rho} + \frac{\delta E_{xc}[\rho]}{\delta \rho} + \mu_s - \mu \quad (2.11)$$



Since the Kohn-Sham reference frame is a non-interacting system, we can write the Schrodinger equation for each orbital as

$$\left\{-\frac{\nabla^2}{2} + V_{eff}(\vec{r})\right\}\phi_i(\vec{r}) = \epsilon_i\phi_i(\vec{r}) \quad (2.12)$$

along with the relation between electronic density and orbital

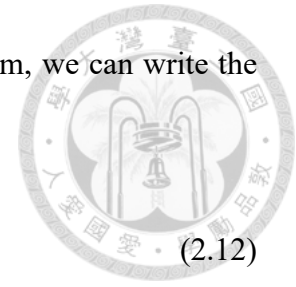
$$\rho(\vec{r}) = \sum_{i=1}^N |\phi_i(\vec{r})|^2 \quad (2.13)$$

we can get a new electronic density $\rho_{new}(\vec{r})$ from the effective potential $V_{eff}(\vec{r})$.

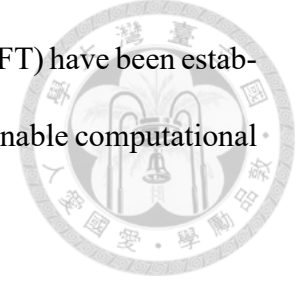
From the relations above, we can get a new electronic density from a given "guessed" electronic density, we will repeat this process in KS-DFT. First, we need to have a guessed density. Then, we obtain a new density from the previous density. After that, we check if the new density is the same as the previous one. If the electronic density is the same self-consistent is achieved; if not we will take the new density as the guessed density and repeat the process until self-consistent. With the electronic density being determined we can then use the density to obtain other properties we wanted.

2.2 Thermally-assisted-occupation density functional theory

While KS-DFT is one of the most used electronic structure calculation methods, it has some shortcomings. For instance, it did not perform well when it come to Strong correlated systems (i.e. multi-reference systems). The approach to treat electrons not interacting with each other help reduce the calculation complexity; however, it comes with some price. We can write the wave function for non-interacting systems as a single Slater determinant hence the difficulty dealing with the multi-reference systems.



Thermally-assisted-occupation density functional theory (TAO-DFT) have been established, and it can deal with those strong correlated systems with reasonable computational cost.[6][7]



In KS-DFT the electron density is

$$\rho(r) = \sum_{i=1}^N |\phi_i(r)|^2 \quad (2.14)$$

In TAO-DFT the electron density is

$$\rho(r) = \sum_{i=1}^{\infty} f_i |\phi_i(r)|^2 \quad (2.15)$$

and the occupation number f_i follow the Fermi-Dirac distribution

$$f_i = \frac{1}{1 + \exp[(\epsilon_i - \mu)/\theta]} \quad (2.16)$$

where θ is the fictitious temperature, ϵ_i is the orbital energy. And f_i will satisfied

$$\sum_{i=1}^{\infty} f_i = N \quad (2.17)$$

and

$$0 \leq f_i \leq 1$$

where N is the number of electron.

In TAO-DFT the energy functional is

$$E[\rho] = \int \rho(\vec{r}) V_{ext}(\vec{r}) d\vec{r} + F[\rho] \quad (2.18)$$

and we can write $F[\rho]$ as

$$F[\rho] = A_S^\theta[\rho] + E_H[\rho] + E_{xc}[\rho] + E_\theta[\rho] \quad (2.19)$$

Here $A_S^\theta[\rho]$ is the kinetic free energy of non interacting system with temperature being θ . And $E_\theta[\rho]$ is the kinetic free energy difference between temperature being zero and θ ,

$E_\theta[\rho] \equiv T_s[\rho] - A_S^\theta[\rho] = A_S^{\theta=0}[\rho] - A_S^\theta[\rho]$. Therefore, we can get the Euler equation

$$\mu = \frac{\delta E[\rho]}{\delta \rho} = V_{ext}(\vec{r}) + \frac{\delta A_S^\theta[\rho]}{\delta \rho} + \frac{\delta E_H[\rho]}{\delta \rho} + \frac{\delta E_{xc}[\rho]}{\delta \rho} + \frac{\delta E_\theta[\rho]}{\delta \rho} \quad (2.20)$$

We consider an auxiliary system in which electrons are non interacting and moving under a potential $V_S(\vec{r})$ at a temperature of θ . By dealing with grand canonical potential, we can get Euler equation for ρ_S , the thermal equilibrium density.

$$\mu_S = \frac{\delta A_S^\theta[\rho_S]}{\delta \rho_S} + V_S(\vec{r}) \quad (2.21)$$

For ρ_S to be the same as ρ , from the two Euler equations above we can get

$$V_S(\vec{r}) = V_{ext}(\vec{r}) + \frac{\delta E_H[\rho]}{\delta \rho} + \frac{\delta E_{xc}[\rho]}{\delta \rho} + \frac{\delta E_\theta[\rho]}{\delta \rho} + \mu_S - \mu \quad (2.22)$$

In the auxiliary system we can also write the Schrodinger equation

$$\left\{ -\frac{\nabla^2}{2} + V_S(\vec{r}) \right\} \phi_i(\vec{r}) = \epsilon_i \phi_i(\vec{r}) \quad (2.23)$$

and the electron density

$$\rho(\vec{r}) = \rho_S(\vec{r}) = \sum_{i=1}^{\infty} f_i |\phi_i(\vec{r})|^2 \quad (2.24)$$

we get the occupation number f_i followed the Fermi-Dirac distribution

$$f_i = \frac{1}{1 + \exp[(\epsilon_i - \mu)/\theta]} \quad (2.25)$$

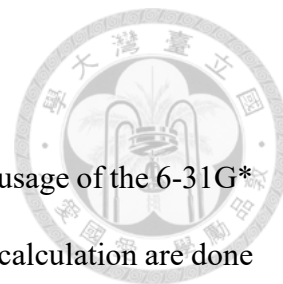
and μ is chosen to make the number of electron number conserved

$$\sum_{i=1}^{\infty} f_i = N \quad (2.26)$$

From the above equations (2.21 - 2.26) we also get an self-consistent process to get the ground state electron density similar to KS-DFT. Start with a "guessed" trial density $\rho_t(\vec{r})$ to get $V_S(\vec{r})$, then using the Schrodinger equation to get $\{\epsilon_i, \phi_i(\vec{r})\}$. Next, from the conserved of the number of electron we can find μ and then $\{f_i\}$. Finally we will have an new electron density $\rho(\vec{r})$ to check if it is converged with the trial density.

2.3 Computational detail

All DFT calculations in our study are run by Q-Chem 4.4, with the usage of the 6-31G* basic set, which is a valence double-zeta polarized basis set.[12] The calculation are done by TAO-DFT with the local density approximation exchange correlation, we will refer to it as TAO-LDA. The fictitious temperature θ are set to be 7 mhartree.





Chapter 3

Results

There are various types of xanthophylls exist in the world, we put our interest in four types of xanthophylls with common usage in research and industry: astaxanthin, canthaxanthin, lutein, zeaxanthin. From the result of TAO-DFT calculation, we find that these four all have significant radical nature. To explore more on their radical nature and the effect on the electronic properties, we put our focus on their counterpart with a longer polyene chain. To have a better understanding of our chosen methodology of lengthening xanthophylls, please check Figure 3.1. In the figure, there is the structure of normal lutein (40-lutein) and its counterparts with more carbon atoms in its conjugated carbon bond (50-lutein and 60-lutein). To lengthen xanthophylls, we keep their terminal groups the same with a symmetrically lengthen polyene chain by adding ten carbon atoms at a time, which means the number of carbon atoms (n) has a minimum value of 40 and an increment of 10. In the following we will denote these compounds as n -xanthophylls or n -astaxanthin, n -canthaxanthin, n -lutein, n -zeaxanthin referring to specific types of xanthophylls, where n is the carbon number, it indicate the number of carbon atoms in the compound ($n=40,50,60\dots$). The nature forms of the four types of xanthophylls all have

forty carbon atoms ($n=40$), while n -xanthophylls with n greater than or equal to fifty ($n \geq 50$) are their lengthen counterparts.

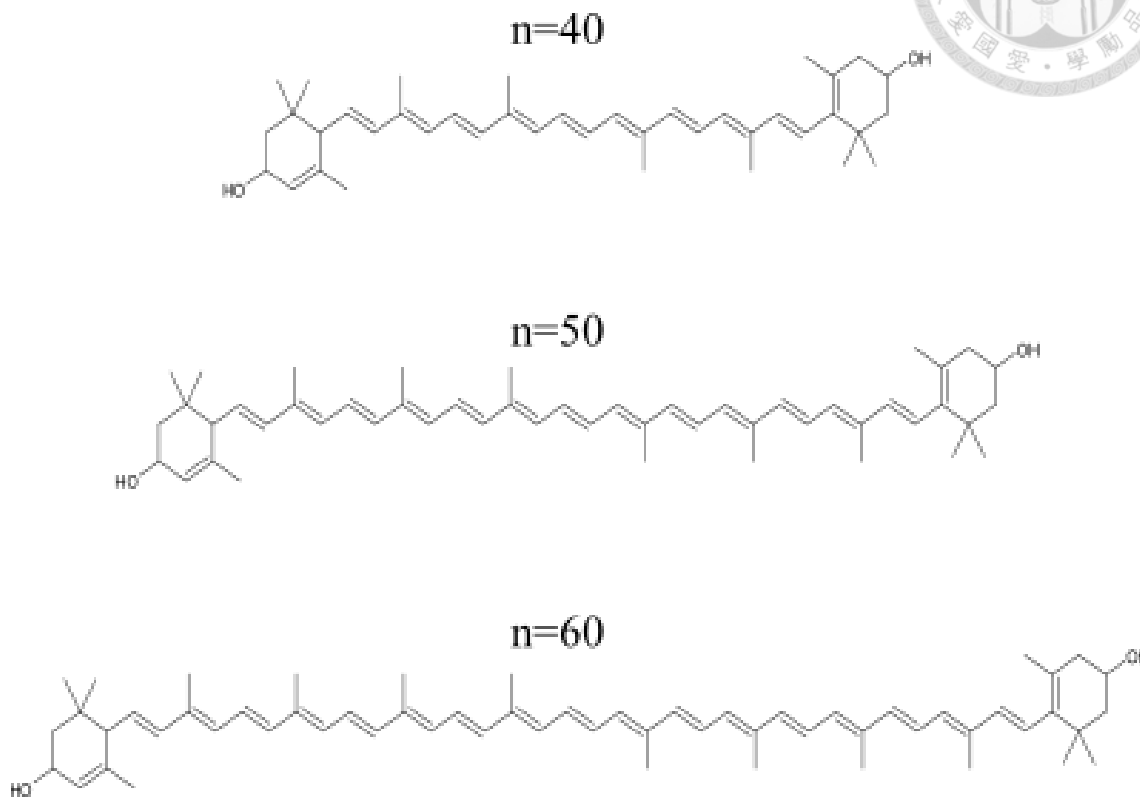


Figure 3.1: The structure of n -lutein with n being the carbon number

There are many carbon-carbon double bonds existing in the structure of xanthophylls, which make xanthophylls have geometric isomerism. Due to the number of double bonds, it would be hard to discuss every possible isomer. For the following, we only perform DFT calculation to two geometric isomers for each xanthophyll, we denoted them as *cis*- n -xanthophyll and *trans*- n -xanthophyll. Consider the connecting part of terminal groups with the carbon bond, it would cause geometric isomer in both ends of n -astaxanthin, n -canthaxanthin, and n -zeaxanthin; while it would only cause geometric isomer in one end of n -lutein. For the isomer, *cis*- n -xanthophylls are *cis* in all the ends; and *trans*- n -xanthophylls are *trans* in all the ends. We did not discuss other situations, like *cis* in one end and *trans* in another end, or *cis*-*trans* isomers happening in the carbon double bond.

The structure can be seen in the following figure.

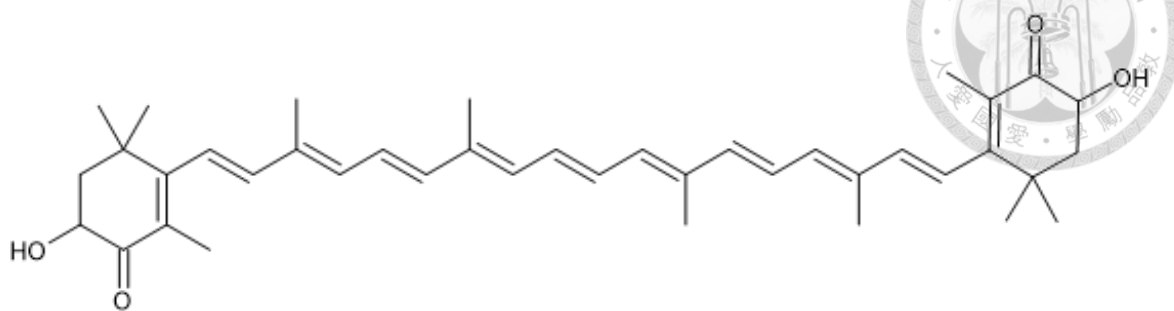


Figure 3.2: The structure of cis-40-astaxanthin

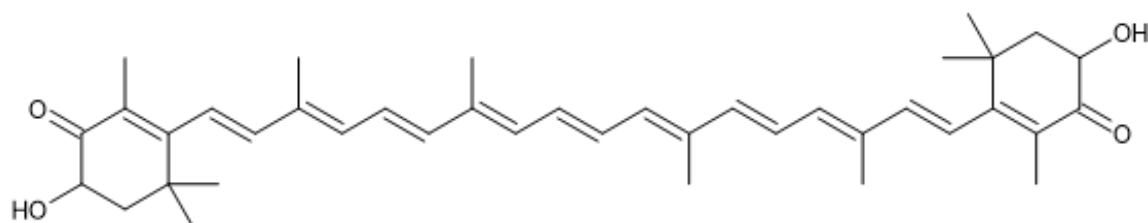


Figure 3.3: The structure of trans-40-astaxanthin

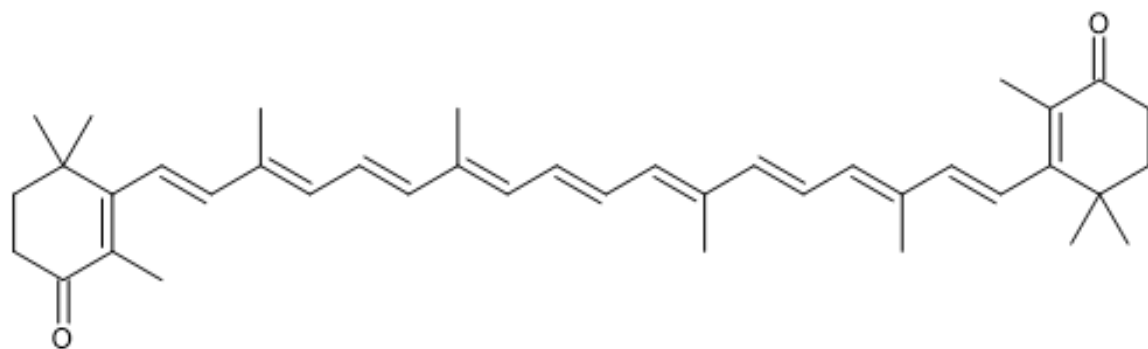


Figure 3.4: The structure of cis-40-canthaxanthin

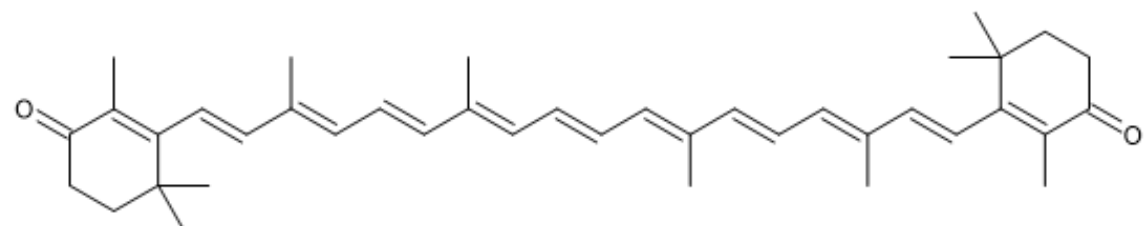


Figure 3.5: The structure of trans-40-canthaxanthin

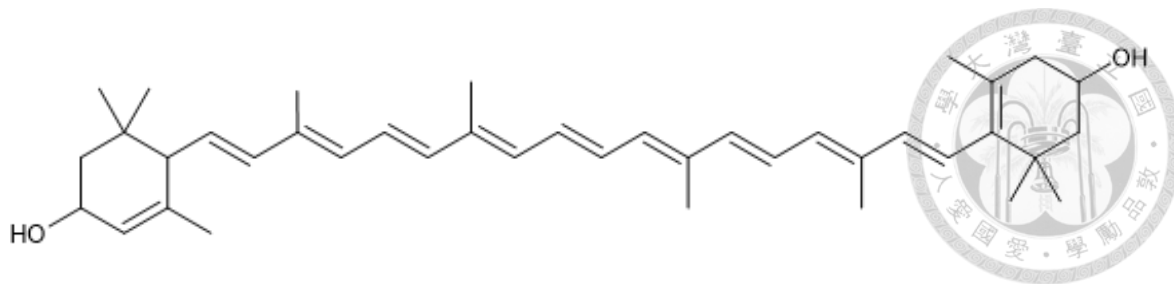


Figure 3.6: The structure of cis-40-lutein

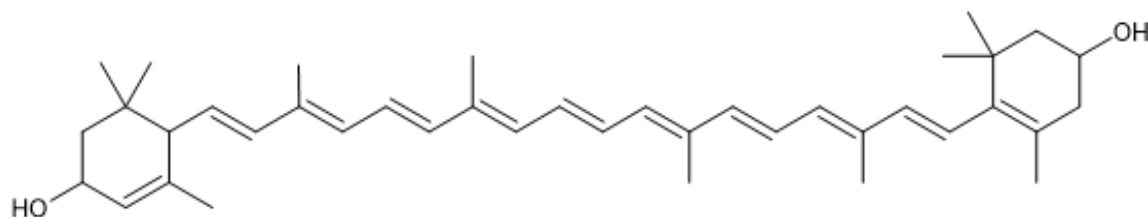


Figure 3.7: The structure of trans-40-lutein

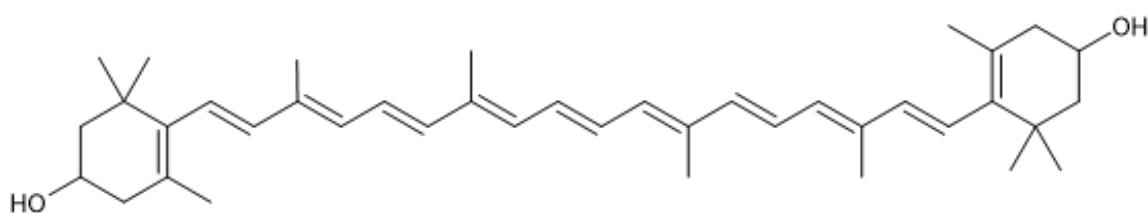


Figure 3.8: The structure of cis-40-zeaxanthin

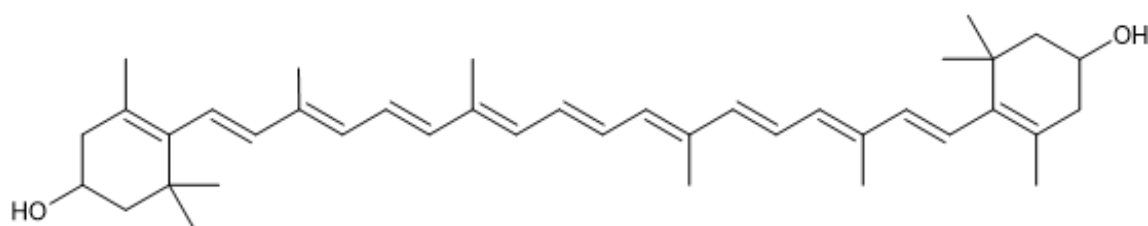
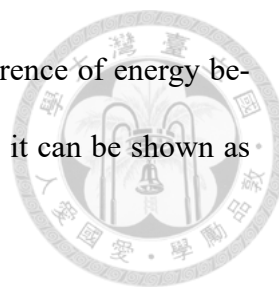


Figure 3.9: The structure of trans-40-zeaxanthin

3.1 Singlet-Triplet gap

We want to know which is the ground state of n-xanthophylls: singlet state or triplet state. Therefore, we performed DFT calculation on both singlet and triplet state to obtain



their respectively ground state energy, hence we can obtain the difference of energy between single and triplet state. We call the energy difference ST gap, it can be shown as following,

$$\text{ST gaps} = E_{\text{triplet}} - E_{\text{singlet}} \quad (3.1)$$

We plot the ST gap for different number of carbon atoms (n) in the following two figure for cis-n-xanthophylls and trans-n-xanthophylls respectively. We can see that for all the xanthophylls here, ST gap are always positive; therefore, we know that singlet state will be the ground state between singlet and triplet state. And that the energy difference monotonically decrease alongside the increase of n.

ST gap for 40-xanthophyll is around 15 to 18 kcal/mol, the energy difference become smaller and come down to about 6 kcal/mol for n-xanthophylls with n larger than 100.

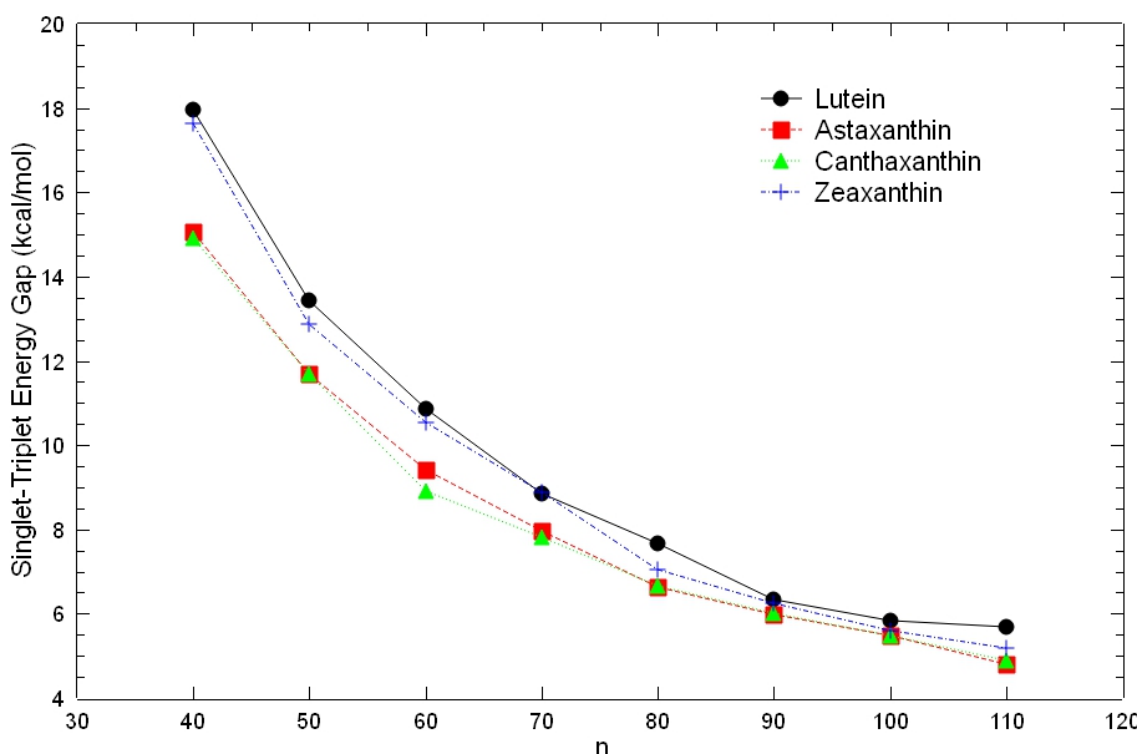


Figure 3.10: Singlet-triplet energy gap of cis-n-xanthophyll with n being the carbon number. We performed the calculations with spin-unrestricted TAO-LDA. The basis set is 6-31G*.

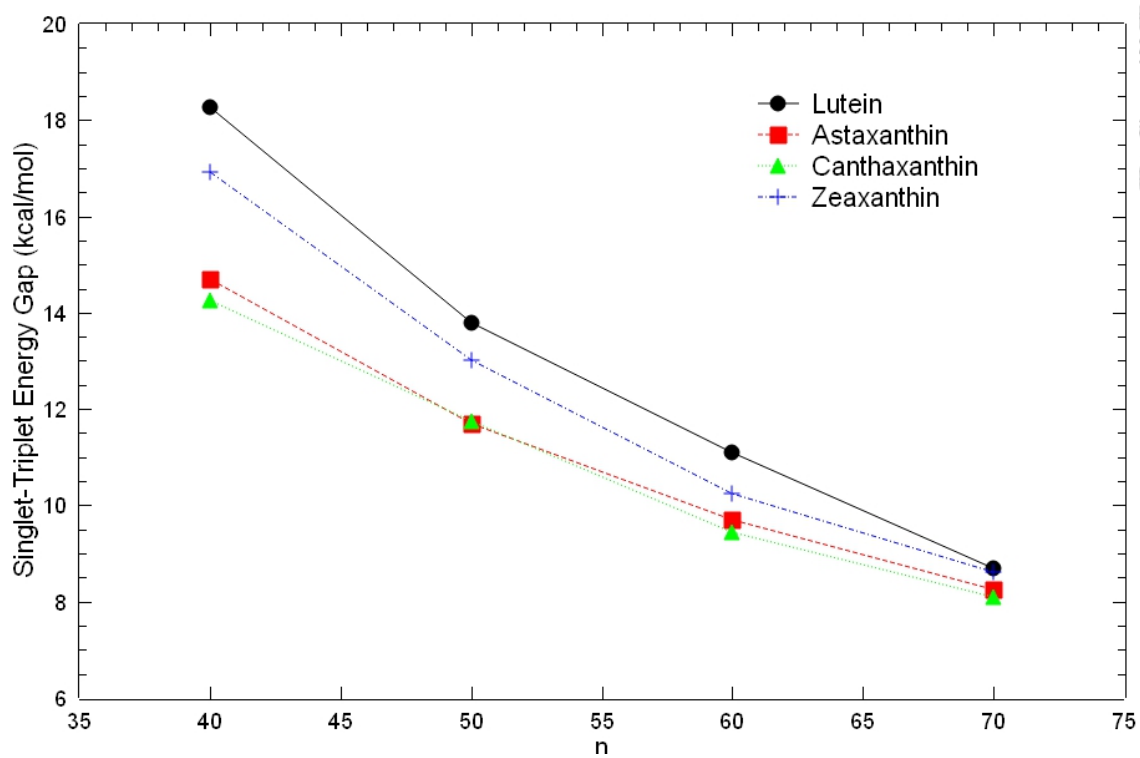


Figure 3.11: Singlet-triplet energy gap of trans-n-xanthophyll with n being the carbon number. We performed the calculations with spin-unrestricted TAO-LDA. The basis set is 6-31G*.

For cis-n-xanthophyll, the value of singlet and triplet state energy and the ST-gap are display in the following two tables. From the table we can see that the energy of cis-n-lutein and cis-n-zeaxanthin are very close (difference is under 0.001 %) in the same circumstance, while cis-n-canthaxanthin have a small difference (under 0.02 %), and cis-n-astaxanthin have a large difference(over 3 %). It is because cis-n-lutein and cis-n-zeaxanthin have a similar structure and the same molecular formula, while cis-n-astaxanthin have more oxygen atoms compare to other three types of xanthophyll.

n	cis-n-astaxanthin			cis-n-canthaxanthin		
	Singlet state	Triplet state	ST-gap	Singlet state	Triplet state	ST-gap
40	-1839.74	-1839.71	15.05	-1690.35	-1690.33	14.92
50	-2224.37	-2224.35	11.68	-2074.99	-2074.97	11.69
60	-2609.00	-2608.99	9.41	-2459.63	-2459.61	10.30
70	-2993.64	-2993.63	7.96	-2844.26	-2844.25	7.83
80	-3378.27	-3378.26	6.64	-3228.90	-3228.89	6.67
90	-3762.91	-3762.90	5.97	-3613.53	-3613.52	6.01
100	-4147.54	-4174.54	5.48	-3998.17	-3998.16	5.47
110	-4532.18	-4532.17	4.80	-4382.80	-4382.80	4.89

Table 3.1: Singlet and triplet state energy (Hartee) and the ST-gap (kcal/mol) for cis-n-astaxanthin and cis-n-canthaxanthin, where n is the carbon number. We performed the calculations with spin-unrestricted TAO-LDA. The basis set is 6-31G*.

n	cis-n-lutein			cis-n-zeaxanthin		
	Singlet state	Triplet state	ST-gap	Singlet state	Triplet state	ST-gap
40	-1692.66	-1692.64	17.96	-1692.68	-1692.65	17.63
50	-2077.30	-2077.28	13.44	-2077.31	-2077.29	12.87
60	-2461.93	-2461.92	10.87	-2461.95	-2461.93	10.53
70	-2846.57	-2846.56	8.84	-2844.26	-2844.25	7.83
80	-3231.21	-3231.19	8.07	-3231.22	-3231.20	7.05
90	-3615.84	-3615.83	6.34	-3615.85	-3615.84	6.26
100	-4000.48	-4000.47	5.83	-4000.49	-4000.48	5.60
110	-4385.11	-4385.10	5.69	-4385.12	-4385.11	5.19

Table 3.2: Singlet and triplet state energy (Hartee) and the ST-gap (kcal/mol) for cis-n-lutein and cis-n-zeaxanthin, where n is the carbon number. We performed the calculations with spin-unrestricted TAO-LDA. The basis set is 6-31G*.

3.2 Energy difference between cis–trans isomerism

The structure of xanthophylls lead to the exist of cis-trans isomers, to determine the energy relation between isomers, we performed DFT calculation on cis-n-xanthophyll and trans-n-xanthophyll to obtain their ground state energy; hence the energy difference. The energy gap is define as the following,

$$\text{Cis – Trans isomer energy gaps} = E_{\text{cis-isomer}} - E_{\text{trans-isomer}} \quad (3.2)$$

We plot the energy gap for different number of carbon atoms (n) in the following figure. For all the xanthophylls here, only n-astaxanthin with n>40 have a large energy

difference which is slightly bigger than 5 kcal/mol between geometric isomers, this value is still smaller than the singlet-triplet energy gap for respective xanthophylls. The ST-gap of n-astaxanthin with n=50, 60, 70 are between 7.96 to 11.68 (kcal/mol). For n-zeaxanthin, only when n=40 the energy gap will be close to zero. For other xanthophylls, they have a positive energy difference less than 1 kcal/mol. Therefore we know that trans-xanthophyll have a lower ground state energy than cis-n-xanthophyll.

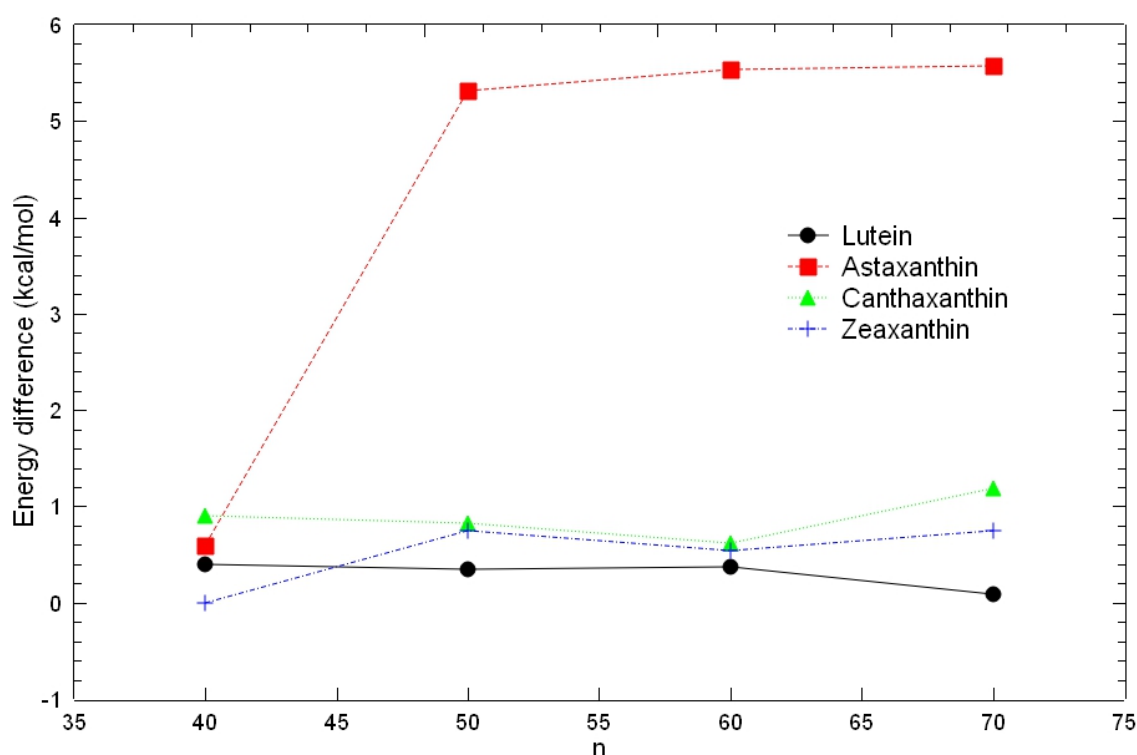


Figure 3.12: Singlet state energy difference between cis-n-xanthophyll and trans-n-xanthophyll with n being the carbon number. We performed the calculations with spin-unrestricted TAO-LDA. The basis set is 6-31G*.

3.3 Vertical ionization potential & Vertical electron affinity & Fundamental gap



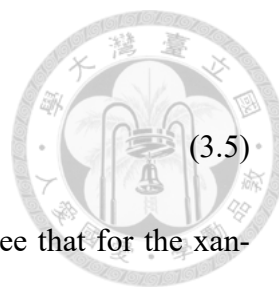
From previous result we know that between singlet state and triplet state the ground state will be singlet state, so for the following section we will focus on singlet state n-xanthophyll.

We perform the calculation to obtain vertical ionization potential (IP_V), vertical electron affinity (EA_V) and fundamental gap (E_g). IP_V is the energy required when we removed an electron from the compound with the geometry remain the same; EA_V is the energy released when we add an electron to the compound with the geometry of atoms remain the same ;and E_g is the difference between vertical ionization potential and vertical electron affinity.[11]

We use the upper-case N to represent the number of electrons in the neutral xanthophylls, the lower-case n represent the number of carbon atoms of the xanthophylls. Consequently, we can use E_{N+1} , E_N , E_{N-1} to indicate the energy of n-xanthophyll with the number of electrons being N+1,N,N-1 respectively with the geometry remain the same from the ground state neutral n-xanthophyll, which have N electrons. As a result we can express vertical ionization potential (IP_V), vertical electron affinity (EA_V) and fundamental gap (E_g) as the following form.

$$IP_V = E_{N-1} - E_N \quad (3.3)$$

$$EA_V = E_N - E_{N+1} \quad (3.4)$$



$$E_g = IP_V - EA_V = E_{N+1} + E_{N-1} - 2E_N \quad (3.5)$$

We plot these three property in the following figures. We can see that for the xanthophylls here, with the the number of carbon atom in the carbon bond increasing, IP_V monotonically decreasing and EA_V monotonically increasing ; therefore, E_g decreasing as a result.

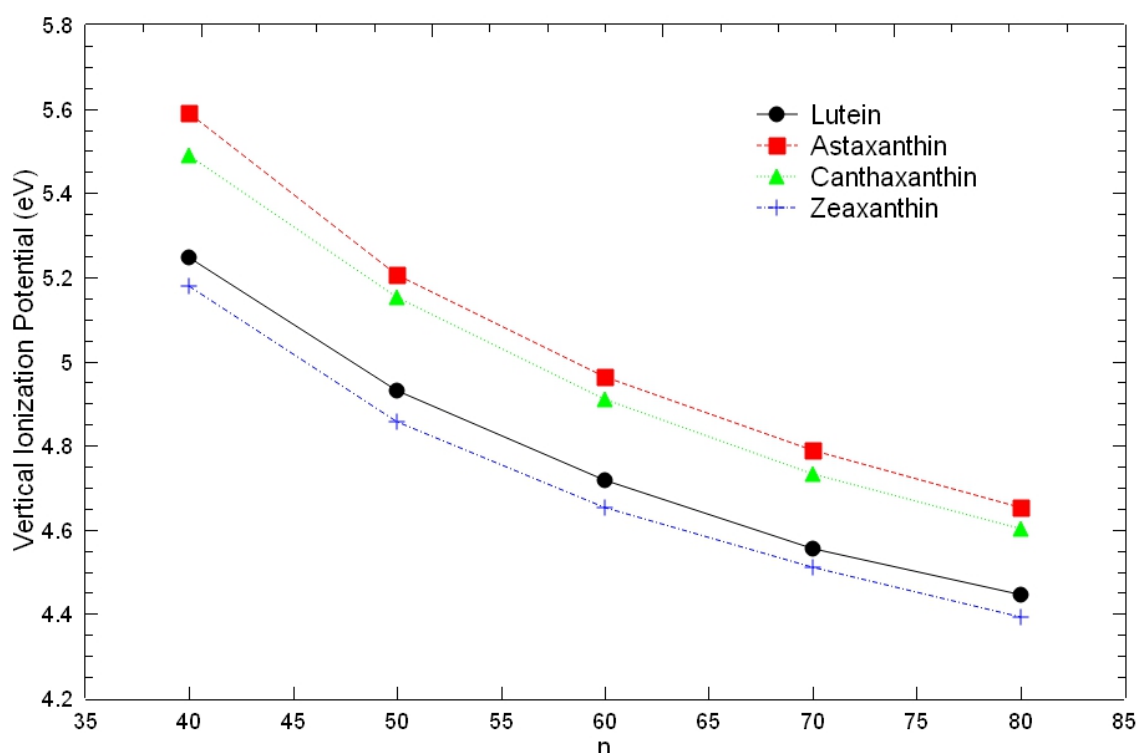


Figure 3.13: Vertical ionization potential of cis-n-xanthophyll with n being the carbon number. We performed the calculations with spin-unrestricted TAO-LDA. The basis set is 6-31G*.

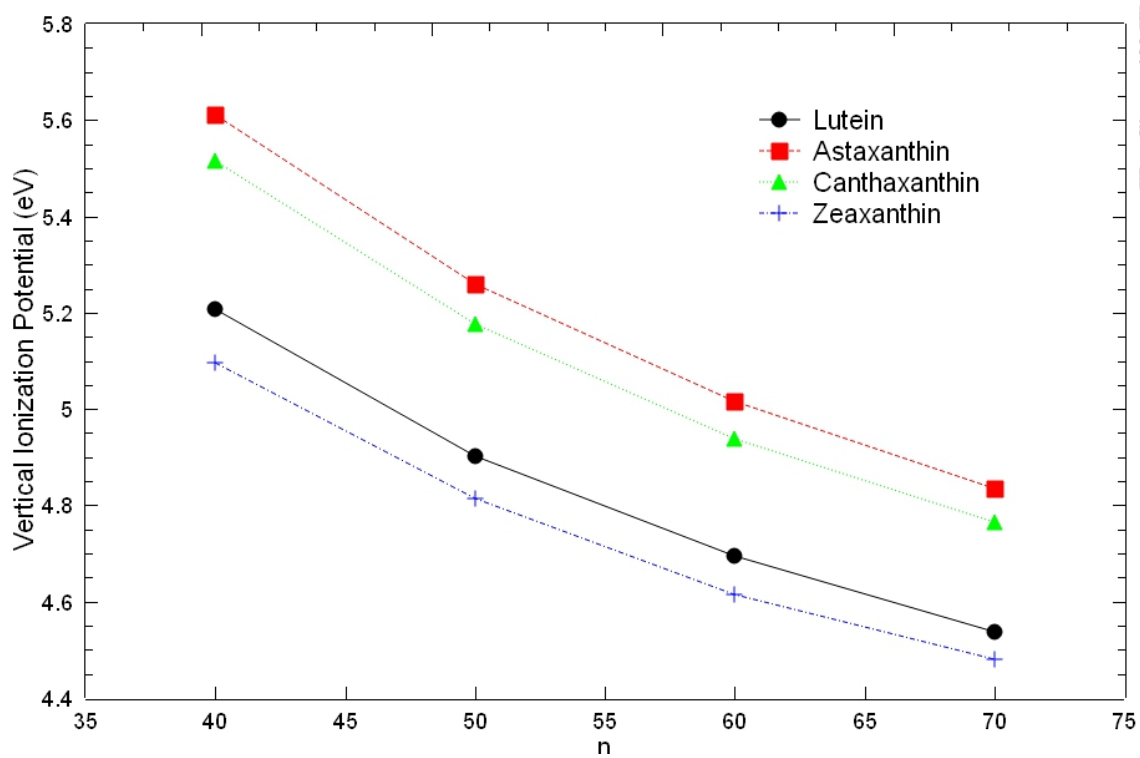


Figure 3.14: Vertical ionization potential of trans-n-xanthophyll with n being the carbon number. We performed the calculations with spin-unrestricted TAO-LDA. The basis set is 6-31G*.

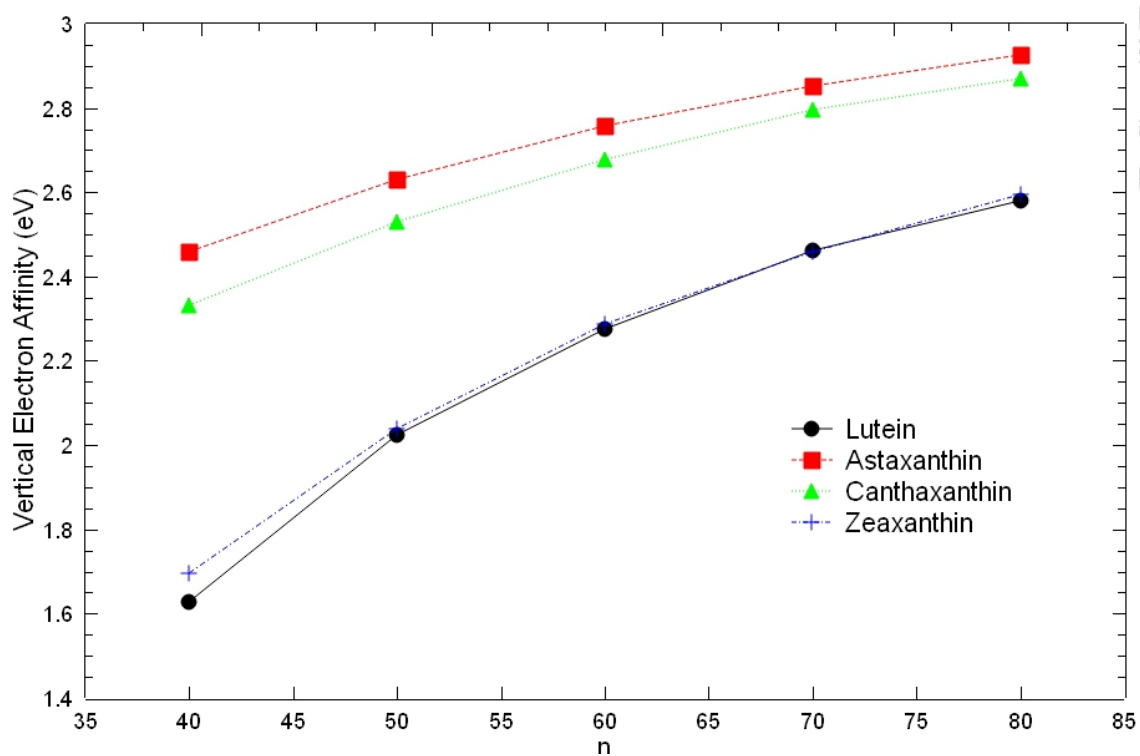


Figure 3.15: Vertical electron affinity of *cis*-*n*-xanthophyll with *n* being the carbon number. We performed the calculations with spin-unrestricted TAO-LDA. The basis set is 6-31G*.

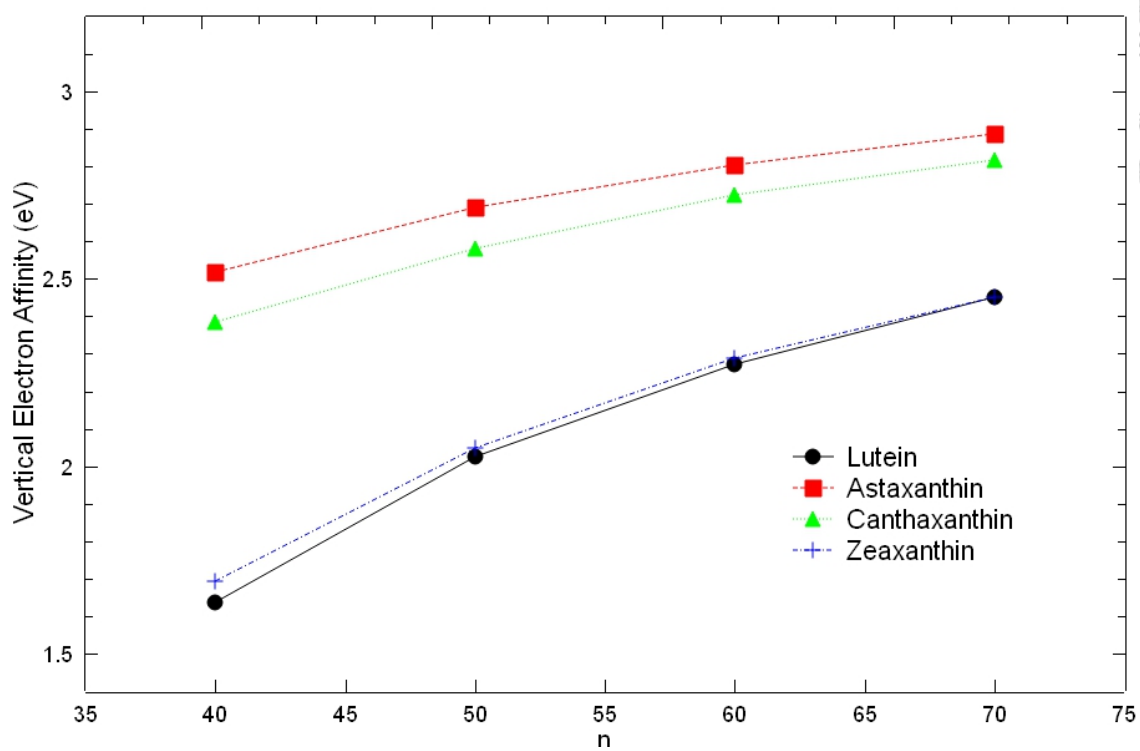


Figure 3.16: Vertical electron affinity of trans-n-xanthophyll with n being the carbon number. We performed the calculations with spin-unrestricted TAO-LDA. The basis set is 6-31G*.

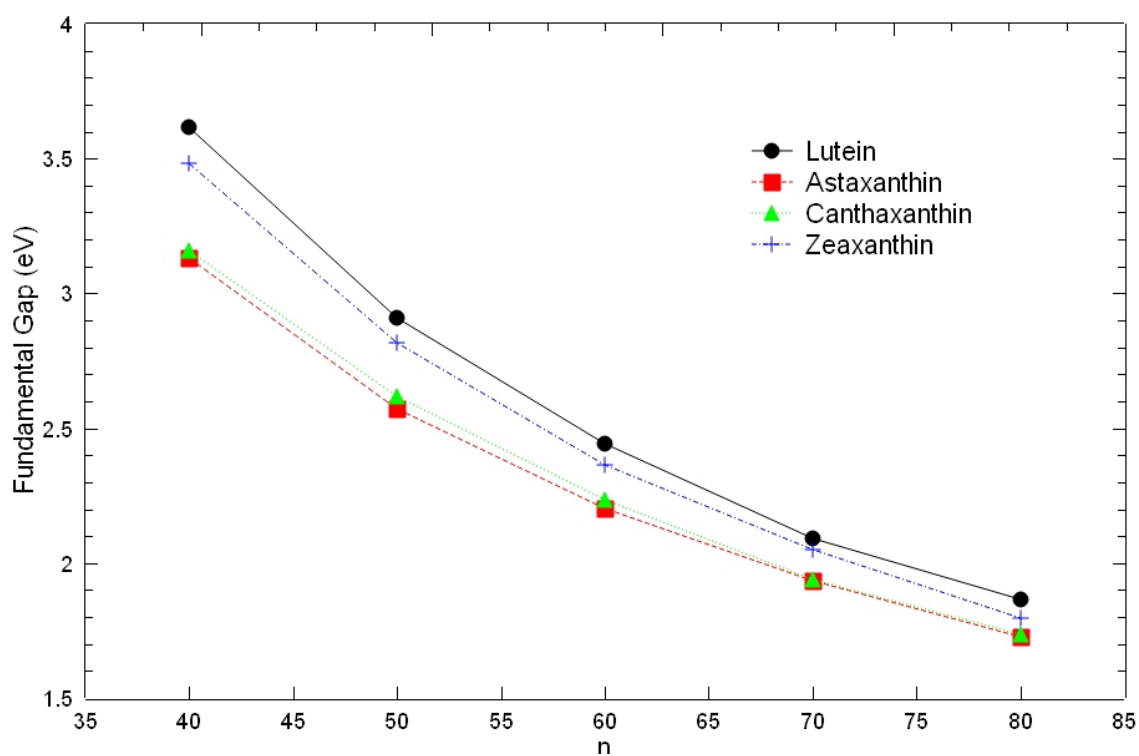


Figure 3.17: Fundamental gap of cis-n-xanthophyll with n being the carbon number. We performed the calculations with spin-unrestricted TAO-LDA. The basis set is 6-31G*.

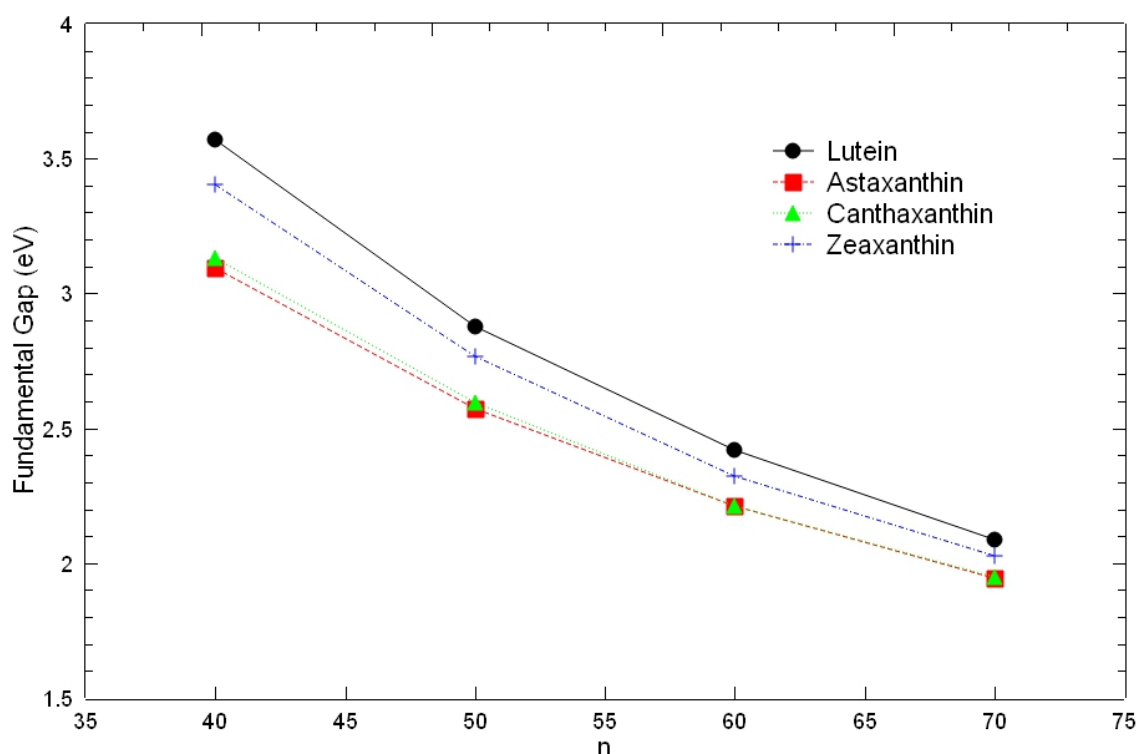


Figure 3.18: Fundamental gap of trans-n-xanthophyll with n being the carbon number. We performed the calculations with spin-unrestricted TAO-LDA. The basis set is 6-31G*.

3.4 Symmetrized von Neumann entropy

To understand the radical nature of xanthophyll, we calculate their symmetrized von Neumann entropy (S_{vN}).

Symmetrized von Neumann entropy is

$$S_{vN} = -\frac{1}{2} \sum_{\sigma=\uparrow\downarrow} \sum_{i=1}^{\infty} \{f_{i,\sigma} \ln(f_{i,\sigma}) + (1 - f_{i,\sigma}) \ln(1 - f_{i,\sigma})\} \quad (3.6)$$

Where $f_{i,\sigma}$ represent the occupation number of i th σ spin orbital. For systems without radical nature, the occupation number of all orbital ($f_{i,\sigma}$) will be close to either 1 or 0 (i.e. $f_{i,\sigma} < 0.1$ or $f_{i,\sigma} > 0.9$). By contrast, for systems with radical nature, there are some orbitals with the occupation number ($f_{i,\sigma}$) far from 1 and 0 (i.e. $0.1 < f_{i,\sigma} < 0.9$). As a

result, S_{vN} for systems without radical nature will be close to zero, while S_{vN} for systems with radical nature will have a much larger value.

We plot the S_{vN} for xanthophyll with different number of carbon atoms (n), from the figure 3.19 and 3.20 we can find that S_{vN} monotonically increase with the increase of the carbon atoms, S_{vN} of 40-xanthophyll are around 0.5 while S_{vN} of 110-xanthophyll are larger than 2. This means that xanthophyll with longer carbon chain will have more significant radical nature.

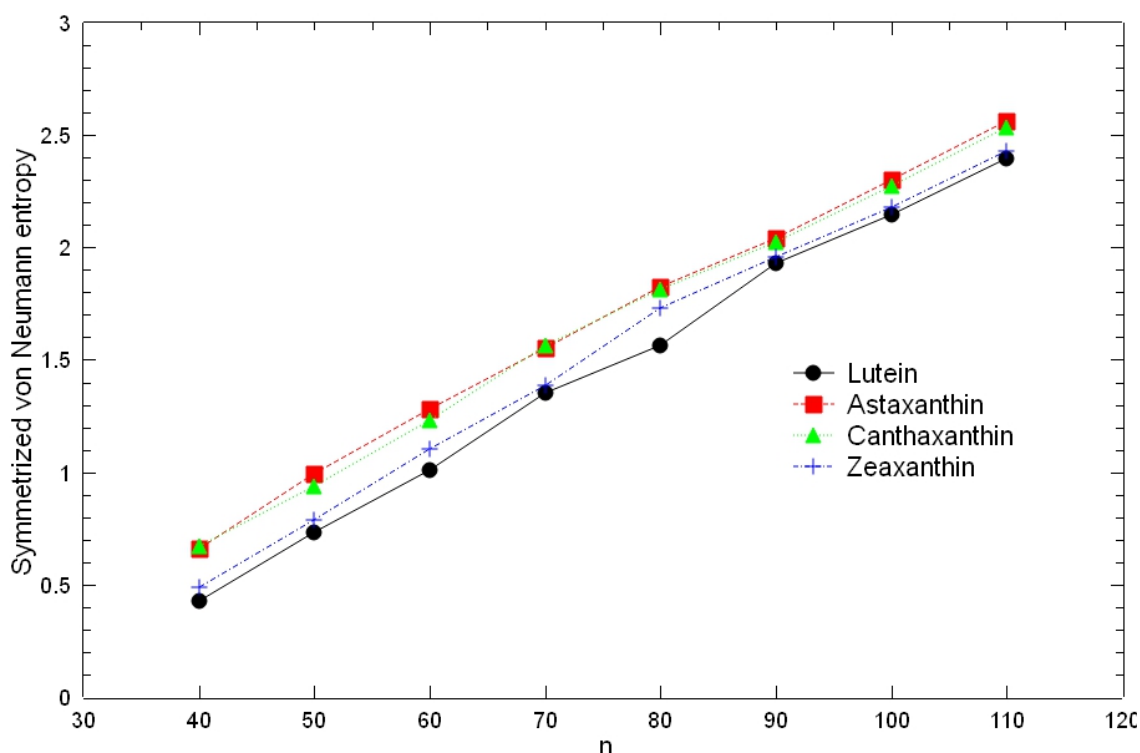


Figure 3.19: Symmetrized von Neumann entropy of cis-n-xanthophyll with n being the carbon number. We performed the calculations with spin-unrestricted TAO-LDA. The basis set is 6-31G*.

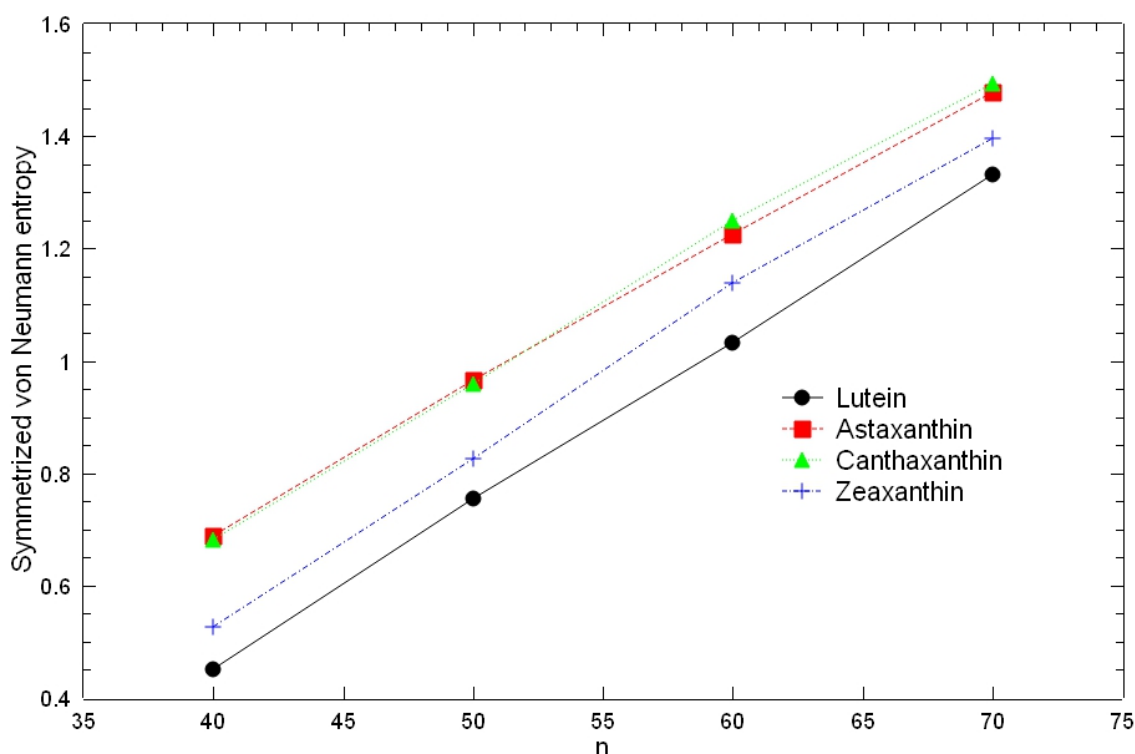


Figure 3.20: Symmetrized von Neumann entropy of trans-n-xanthophyll with n being the carbon number. We performed the calculations with spin-unrestricted TAO-LDA. The basis set is 6-31G*.

3.5 Active orbital occupation numbers

To have a better understanding of the reason behind why S_{vN} monotonically increase with the number of the carbon atoms, we plot the active orbital occupation numbers for different number of carbon atoms (n) in the following figures.

In TAO-DFT the Highest Occupied Molecular Orbital (HOMO) is the $n/2$ th orbital and the Lowest Unoccupied Molecular Orbital (LUMO) is the $n/2+1$ th orbital. The occupation number will be the sum over two spin, hence the maximum value being 2. The orbital occupation number for n-xanthophyll all performed a similar trend. While $n = 40$, the occupation number are either close to 0 or 2 except for HOMO and LUMO, hence the

radical nature for 40-xanthophyll. With the increase of carbon atoms, the occupation number are become closer to 1 including orbital outside HOMO and LUMO. In the case for the largest xanthophyll in our study, 110-xanthophyll, the occupation numbers are the closet to 1, the occupation number for HOMO is less than 1.5 and the occupation number of LUMO is bigger than 0.5, along with the occupation number of HOMO-1 and LUMO+1 are also far from 0 or 2. From the result of occupation numbers, we have a better understanding of the reasoning behind the fact longer xanthophyll have a more significant radical nature. We believe the trend will hold for n-xanthophyll with the number of carbon atoms over 110.

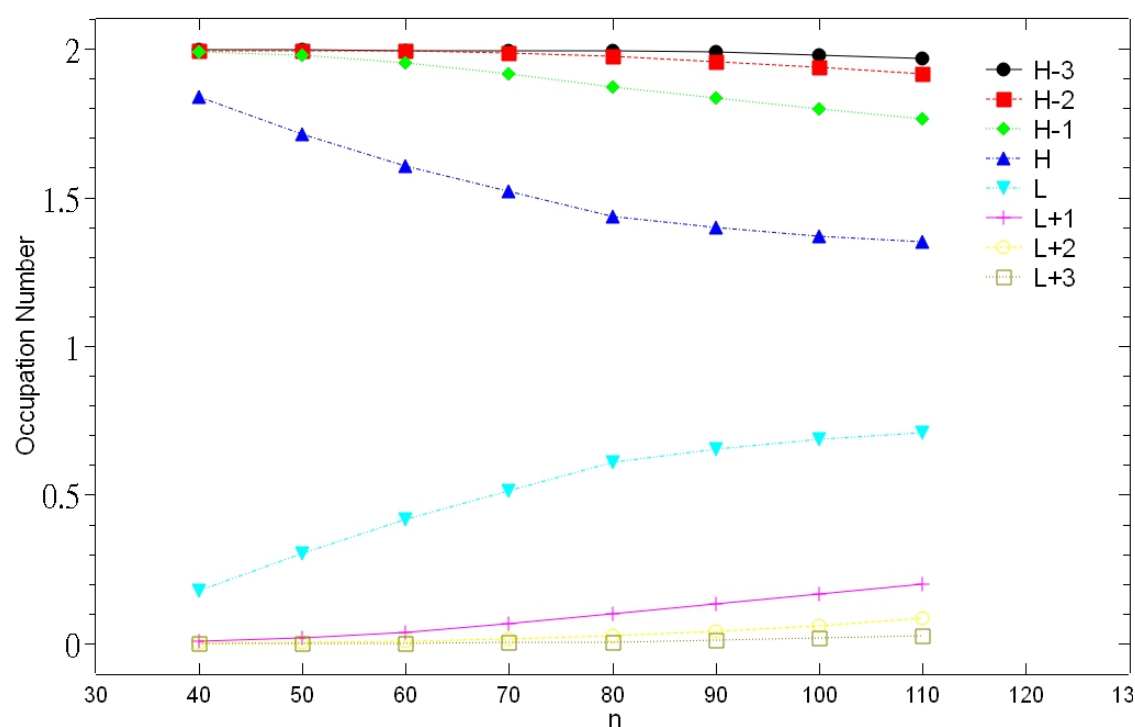


Figure 3.21: Active orbital occupation numbers (HOMO-3, HOMO-2, HOMO-1, HOMO, LUMO, LUMO+1, LUMO+2, LUMO+3) of cis-n-astaxanthin with n being the carbon number. We performed the calculations with spin-restricted TAO-LDA. The basis set is 6-31G*.

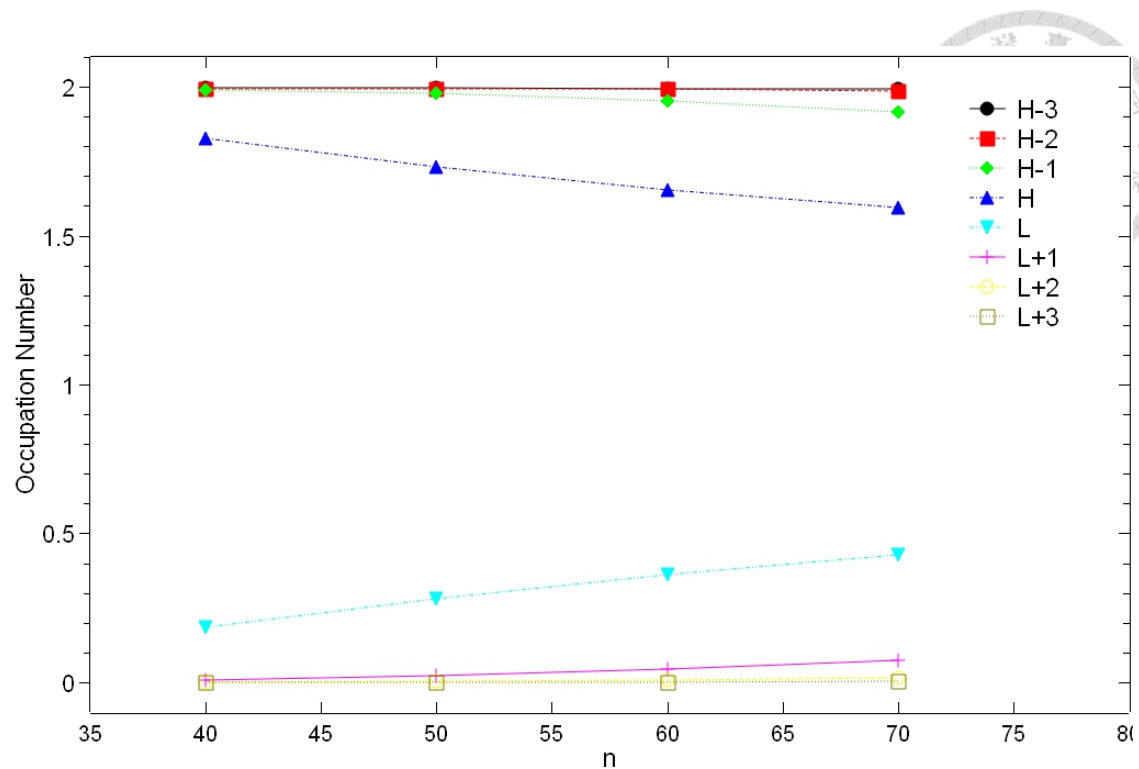


Figure 3.22: Active orbital occupation numbers (HOMO-3, HOMO-2, HOMO-1, HOMO, LUMO, LUMO+1, LUMO+2, LUMO+3) of trans-n-astaxanthin with n being the carbon number. We performed the calculations with spin-restricted TAO-LDA. The basis set is 6-31G*.

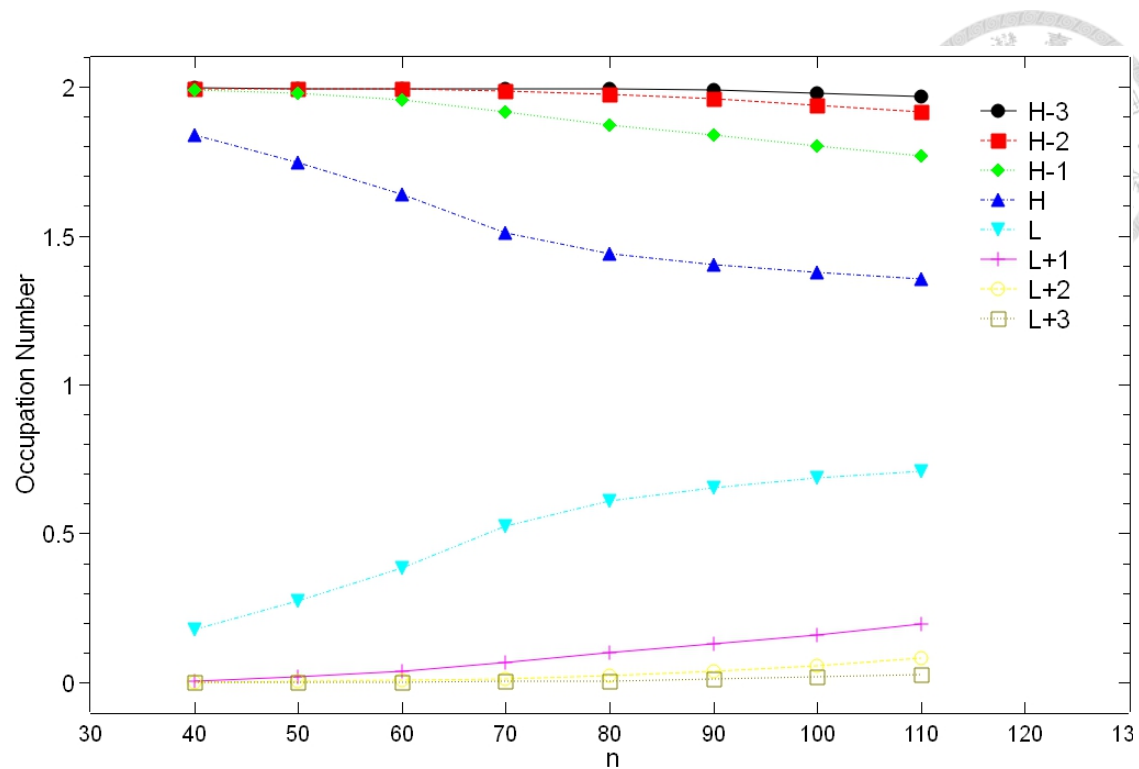


Figure 3.23: Active orbital occupation numbers (HOMO-3, HOMO-2, HOMO-1, HOMO, LUMO, LUMO+1, LUMO+2, LUMO+3) of cis-n-canthalanthin with n being the carbon number. We performed the calculations with spin-restricted TAO-LDA. The basis set is 6-31G*.

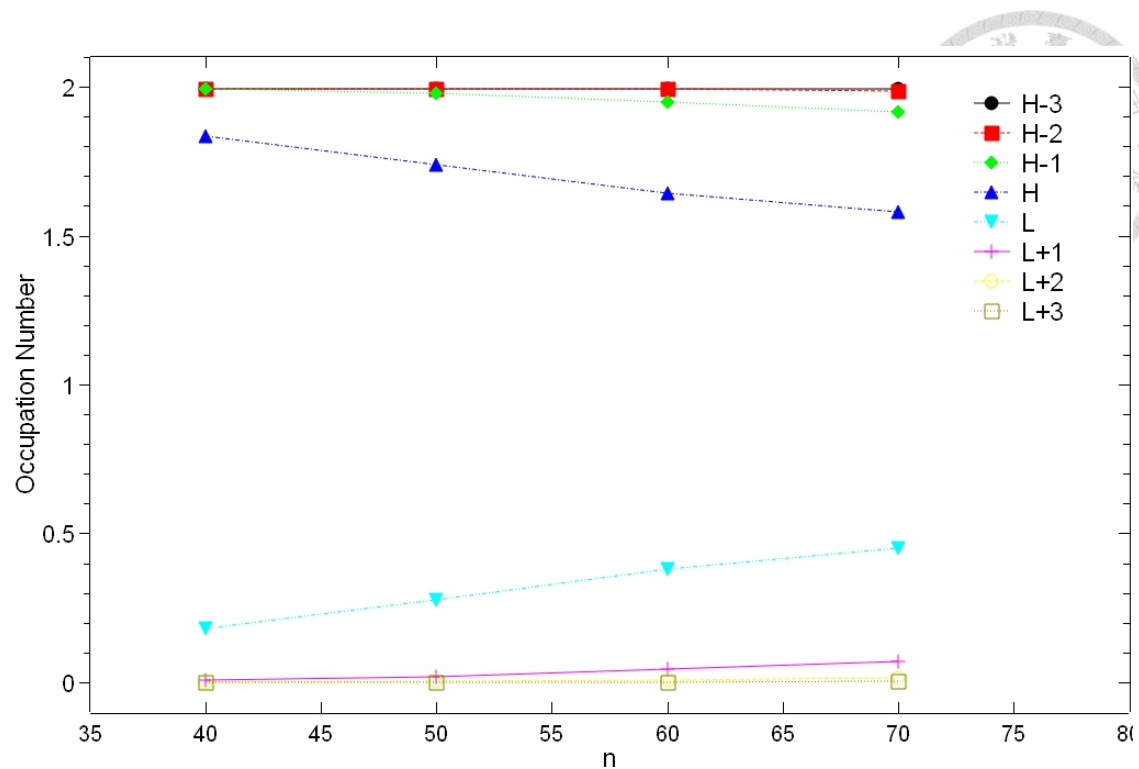


Figure 3.24: Active orbital occupation numbers (HOMO-3, HOMO-2, HOMO-1, HOMO, LUMO, LUMO+1, LUMO+2, LUMO+3) of trans-n-canthaxanthin with n being the carbon number. We performed the calculations with spin-restricted TAO-LDA. The basis set is 6-31G*.

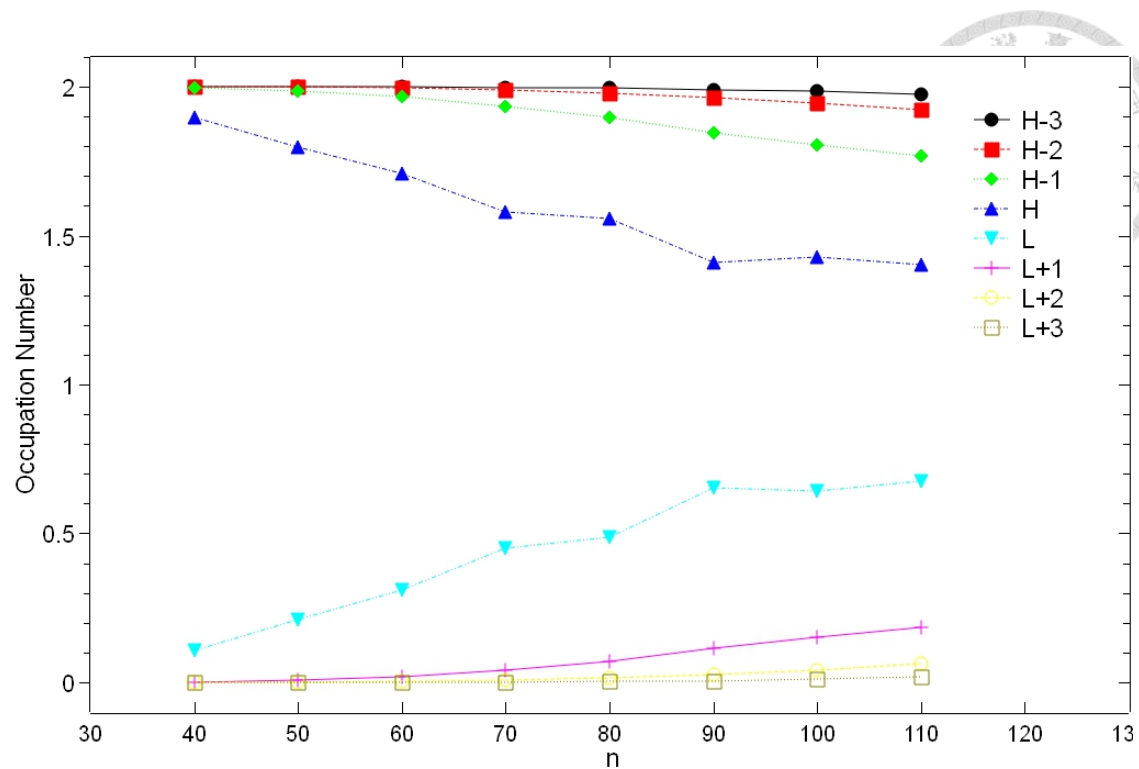


Figure 3.25: Active orbital occupation numbers (HOMO-3, HOMO-2, HOMO-1, HOMO, LUMO, LUMO+1, LUMO+2, LUMO+3) of cis-n-lutein with n being the carbon number. We performed the calculations with spin-restricted TAO-LDA. The basis set is 6-31G*.

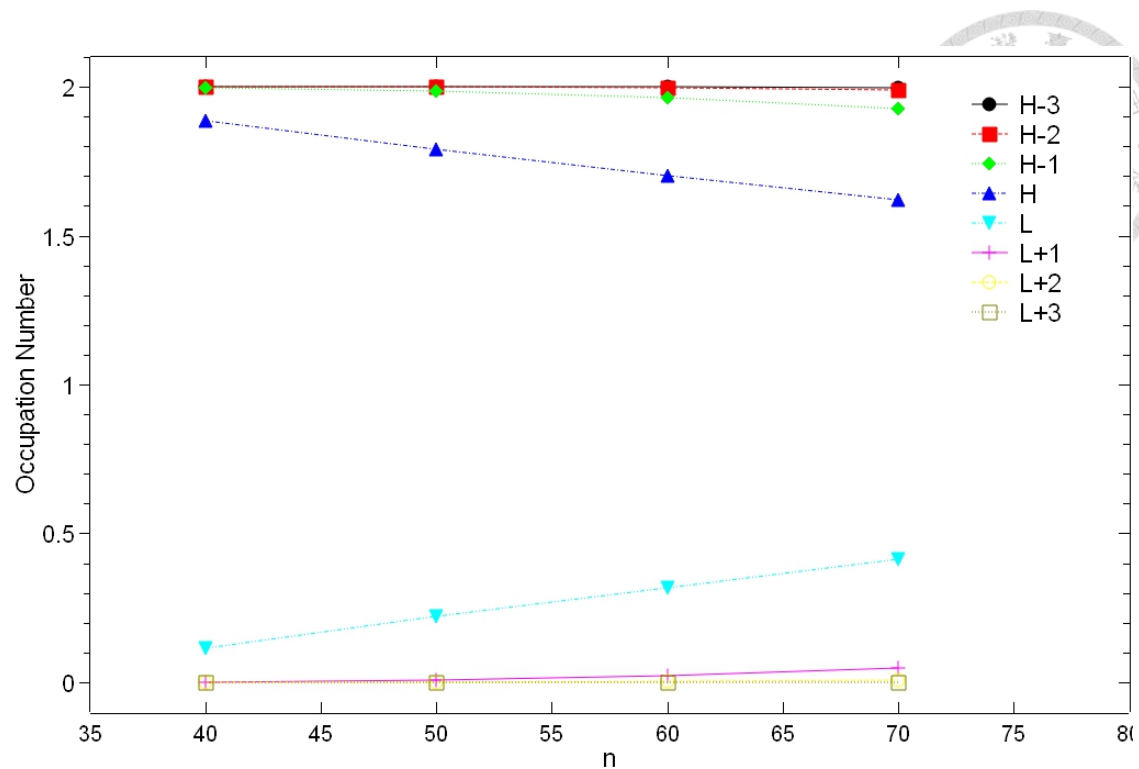


Figure 3.26: Active orbital occupation numbers (HOMO-3, HOMO-2, HOMO-1, HOMO, LUMO, LUMO+1, LUMO+2, LUMO+3) of trans-n-lutein with n being the carbon number. We performed the calculations with spin-restricted TAO-LDA. The basis set is 6-31G*.

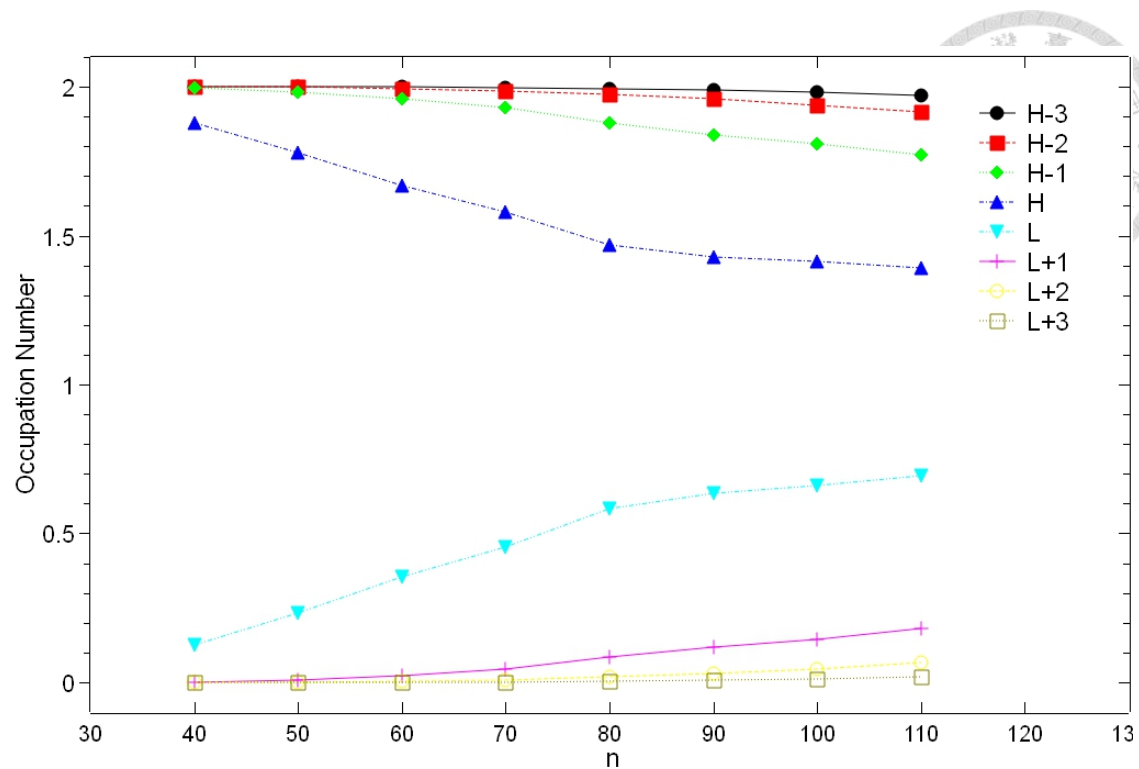


Figure 3.27: Active orbital occupation numbers (HOMO-3, HOMO-2, HOMO-1, HOMO, LUMO, LUMO+1, LUMO+2, LUMO+3) of cis-n-zeaxanthin with n being the carbon number. We performed the calculations with spin-restricted TAO-LDA. The basis set is 6-31G*.

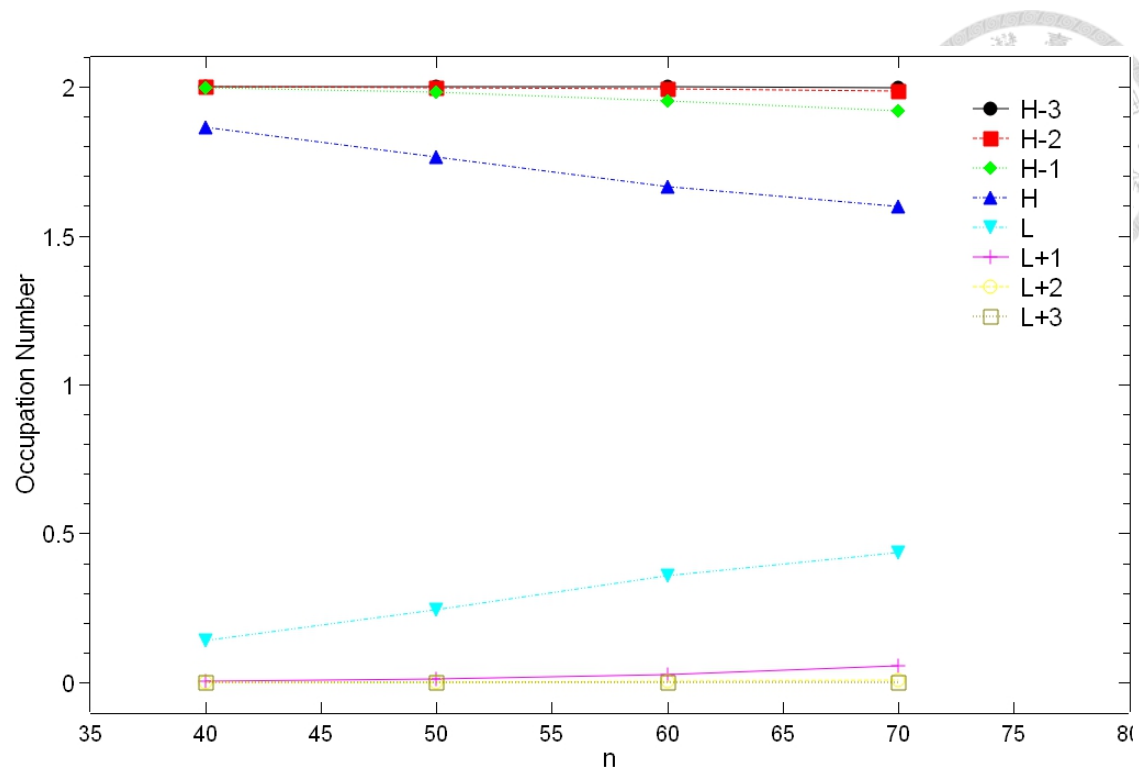


Figure 3.28: Active orbital occupation numbers (HOMO-3, HOMO-2, HOMO-1, HOMO, LUMO, LUMO+1, LUMO+2, LUMO+3) of trans-n-zeaxanthin with n being the carbon number. We performed the calculations with spin-restricted TAO-LDA. The basis set is 6-31G*.



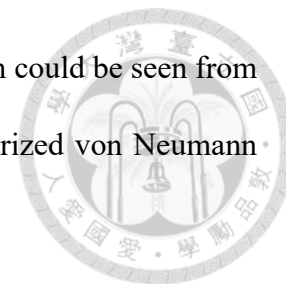
Chapter 4

Summary and future prospect

We performed TAO-LDA calculation on four types of n-xanthophylls (xanthophylls and their related lengthen systems) including n-astaxanthin, n-canthaxanthin, n-lutein, and n-zeaxanthin, to understand their electronic properties and the relation between these properties with the radical nature of xanthophylls. The electronic properties we studied including singlet-triplet gap ($ST\ gaps$), vertical ionization potential (IP_V), vertical electron affinity (EA_V), fundamental gap (E_g), symmetrized von Neumann entropy (S_{vN}), and active orbital occupation numbers. By using TAO-DFT in the study of n-xanthophylls, we could avoid the error that could happen by using KS-DFT to study strong correlated systems. Also, we could avoid the high cost in both time and calculation resources required for other multi-reference methods.

For those n-xanthophylls we studied, we find that the singlet state would be the ground state. The energy difference between cis and trans isomers are negligible except for n-astaxanthin while $n \geq 50$. Vertical ionization potential and the fundamental gap will decrease monotonically as the carbon bond becomes longer; by contrast, vertical electron affinity will increase monotonically. And we also find that the radical nature of n-

xanthophylls will become more significant as n become larger, which could be seen from the result of their active orbital occupation numbers or the symmetrized von Neumann entropy.



In the future, there are some aspect that could be consider to have a more in depth understanding of n -xanthophylls. First, in our study, we did not consider the effect of the environment, we treat xanthophylls as if they exist in the air; however, xanthophylls are often exist as the solute of the solution in the nature, hence the effect of the solvent. Second, if we consider the cis-trans isomer with the isomerism happen in the middle of the carbon double bond, the properties could performed a more different trend. Third, the effect of longer carbon bond with color. Since the carbon bond serve as the chromophore systems, those n -xanthophylls with longer carbon bond could performed very different compare to 40-xanthophylls.

Although those n -xanthophylls are not synthesizable nowadays except for those that exist in nature (n -xanthophylls with $n = 40$), in the study we have a better understanding of them by doing these DFT calculations. With different terminal groups, those four different xanthophylls still have a similar effect regarding the length of the carbon bond. As a result, we could believe that there is a much higher chance that these trend could be applied to more different types of xanthophyll. The gradual increase of the radical nature could be heads-up of the difficulty to synthesize and store n -xanthophylls, which could cause difficulty in the practice.



Reference

- [1] Progress in Carotenoid Research. (2018). (L. Q. Zepka, E. Jacob-Lopes, & V. V. D. Rosso, Eds.). IntechOpen. <https://doi.org/10.5772/intechopen.73775>
- [2] Carotenoids in nature : biosynthesis, regulation and function (2016). (C. Stange, Ed.). Springer International Publishing. <https://doi.org/10.1007/978-3-319-39126-7>
- [3] Britton, George, Liaaen-Jensen, S., & Pfander, H. (1995). *Carotenoids* Birkhäuser Verlag.
- [4] Fernandez-Lopez, J. A., Fernandez-Lledo, V., & Angosto, J. M. (2020). New insights into red plant pigments: more than just natural colorants. *RSC Advances*, 10(41), 24669-24682. <https://doi.org/10.1039/d0ra03514a>
- [5] Seabra, Larissa Mont'Alverne Jucá, Pedrosa, Lucia Fátima Campos. (2010). Astaxanthin: structural and functional aspects. *Revista de Nutrição*, 23(6), 1041-1050. <https://doi.org/10.1590/s1415-52732010000600010>
- [6] Higuera-Ciapara, I., Félix-Valenzuela, L., Goycoolea, F. M. (2006). Astaxanthin: A Review of its Chemistry and Applications. *Critical Reviews in Food Science and Nutrition*, 46(2), 185-196. <https://doi.org/10.1080/10408690590957188>
- [7] Stringham, J. M., & Hammond, B. R. (2005). Dietary lutein and zeaxanthin: Possible effects on visual function. *NUTRITION REVIEWS*, 63(2), 59-64. <https://doi.org/10.1301/nr.2004.feb.59-64>

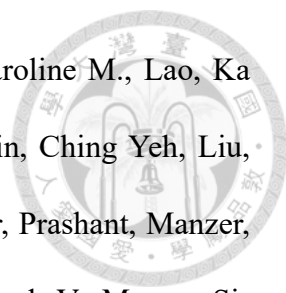
[8] Parr, Robert G., & Yang, Weitao. (1989). *Density-functional theory of atoms and molecules* New York, New York.

[9] Chai, Jeng-Da. (2012). Density functional theory with fractional orbital occupations. *Journal of Chemical Physics*, 136(15), 154104. <https://doi.org/10.1063/1.3703894>

[10] Chai, Jeng-Da. (2014). Thermally-assisted-occupation density functional theory with generalized-gradient approximations. *Journal of Chemical Physics*, 140(18), 18a521. <https://doi.org/10.1063/1.4867532>

[11] Wu, Chun-Shian. Chai, Jeng-Da. (2015). Electronic Properties of Zigzag Graphene Nanoribbons Studied by TAO-DFT. *Journal of Chemical Theory and Computation*, 11(5), 2003-2011. <https://doi.org/10.1021/ct500999m>

[12] Shao, Yihan, Gan, Zhengting, Epifanovsky, Evgeny, Gilbert, Andrew T. B., Wormit, Michael, Kussmann, Joerg, Lange, Adrian W., Behn, Andrew, Deng, Jia, Feng, Xintian, Ghosh, Debashree, Goldey, Matthew, Horn, Paul R., Jacobson, Leif D., Kaliman, Ilya, Khaliullin, Rustam Z., Kuś, Tomasz, Landau, Arie, Liu, Jie, Proynov, Emil I., Rhee, Young Min, Richard, Ryan M., Rohrdanz, Mary A., Steele, Ryan P., Sundstrom, Eric J., Woodcock, H. Lee, Zimmerman, Paul M., Zuev, Dmitry, Albrecht, Ben, Alguire, Ethan, Austin, Brian, Beran, Gregory J. O., Bernard, Yves A., Berquist, Eric, Brandhorst, Kai, Bravaya, Ksenia B., Brown, Shawn T., Casanova, David, Chang, Chun-Min, Chen, Yunqing, Chien, Siu Hung, Closser, Kristina D., Crittenden, Deborah L., Diedenhofen, Michael, DiStasio, Robert A., Do, Hainam, Dutoi, Anthony D., Edgar, Richard G., Fatehi, Shervin, Fusti-Molnar, Laszlo, Ghysels, An, Golubeva-Zadorozhnaya, Anna, Gomes, Joseph, Hanson-Heine, Magnus W. D., Harbach, Philipp H. P., Hauser, Andreas W., Hohenstein, Edward G., Holden, Zachary C., Jagau, Thomas- C., Ji, Hyunjun, Kaduk, Benjamin, Khistyayev, Kirill, Kim, Jaehoon, Kim, Jihan, King, Rollin A.,



Klunzinger, Phil, Kosenkov, Dmytro, Kowalczyk, Tim, Krauter, Caroline M., Lao, Ka Un, Laurent, Adèle D., Lawler, Keith V., Levchenko, Sergey V., Lin, Ching Yeh, Liu, Fenglai, Livshits, Ester, Lochan, Rohini C., Luenser, Arne, Manohar, Prashant, Manzer, Samuel F., Mao, Shan-Ping, Mardirossian, Narbe, Marenich, Aleksandr V., Maurer, Simon A., Mayhall, Nicholas J., Neuscamman, Eric, Oana, C. Melania, Olivares-Amaya, Roberto, O' Neill, Darragh P., Parkhill, John A., Perrine, Trilisa M., Peverati, Roberto, Prociuk, Alexander, Rehn, Dirk R., Rosta, Edina, Russ, Nicholas J., Sharada, Shaama M., Sharma, Sandeep, Small, David W., Sodt, Alexander, Stein, Tamar, Stück, David, Su, Yu-Chuan, Thom, Alex J. W., Tsuchimochi, Takashi, Vanovschi, Vitalii, Vogt, Leslie, Vydrov, Oleg, Wang, Tao, Watson, Mark A., Wenzel, Jan, White, Alec, Williams, Christopher F., Yang, Jun, Yeganeh, Sina, Yost, Shane R., You, Zhi-Qiang, Zhang, Igor Ying, Zhang, Xing, Zhao, Yan, Brooks, Bernard R., Chan, Garnet K. L., Chipman, Daniel M., Cramer, Christopher J., Goddard, William A., Gordon, Mark S., Hehre, Warren J., Klamt, Andreas, Schaefer, Henry F., Schmidt, Michael W., Sherrill, C. David, Truhlar, Donald G., Warshel, Arieh, Xu, Xin, Aspuru-Guzik, Alán, Baer, Roi, Bell, Alexis T., Besley, Nicholas A., Chai, Jeng-Da, Dreuw, Andreas, Dunietz, Barry D., Furlani, Thomas R., Gwaltney, Steven R., Hsu, Chao-Ping, Jung, Yousung, Kong, Jing, Lambrecht, Daniel S., Liang, WanZhen, Ochsenfeld, Christian, Rassolov, Vitaly A., Slipchenko, Lyudmila V., Subotnik, Joseph E., Van Voorhis, Troy, Herbert, John M., Krylov, Anna I., Gill, Peter M. W., Head-Gordon, Martin. (2015). Advances in molecular quantum chemistry contained in the Q-Chem 4 program package. *Molecular Physics*, 113(2), 184-215. <https://doi.org/10.1080/00268976.2014.952696>